Way out there: pathogens, health, and condition of overwintering salmon in the Gulf of Alaska

Christoph M. Deeg[ab]*, **Albina N. Kanzeparova**[c], **Alexei A. Somov**[c], **Svetlana Esenkulova**[b], **Emiliano Di Cicco**[b], **Karia H. Kaukinen**[d], **Amy Tabata**[d], **Tobi J. Ming**[d], **Shaorong Li**[d], **Gideon Mordecai**[e], **Angela Schulze**[d] **and Kristina M. Miller**[ad]

[a]Department of Forest & Conservation Science, University of British Columbia, Vancouver, BC V6T 1Z4, Canada; [b]Pacific Salmon Foundation, Vancouver, BC V6J 4S6, Canada; [c]Pacific branch of VNIRO ("TINRO"), Vladivostok, Russia 690091; [d]Fisheries and Oceans Canada, Pacific Biological Station, Nanaimo, BC V9T 6N7, Canada; [e]Department of Medicine, University of British Columbia, Vancouver, BC V6T 1Z3, Canada

*chrdeeg@gmail.com

Abstract

Salmon are keystone species across the North Pacific, supporting ecosystems, commercial opportunities, and cultural identity. Nevertheless, many wild salmon stocks have experienced significant declines. Salmon restoration efforts focus on fresh and coastal waters, but little is known about the open ocean environment. Here we use high throughput RT-qPCR tools to provide the first report on the health, condition, and infection profile of coho, chum, pink, and sockeye salmon in the Gulf of Alaska during the 2019 winter. We found lower infectious agent number, diversity, and burden compared with coastal British Columbia in all species except coho, which exhibited elevated stock-specific infection profiles. We identified *Loma* sp. and *Ichthyophonus hoferi* as key pathogens, suggesting transmission in the open ocean. Reduced prey availability, potentially linked to change in ocean conditions due to an El Niño event, correlated with energetic deficits and immunosuppression in salmon. Immunosuppressed individuals showed higher relative infection burden and higher prevalence of opportunistic pathogens. We highlight the cumulative effects of infection and environmental stressors on overwintering salmon, establishing a baseline to document the impacts of a changing ocean on salmon.

Key words: Pacific Salmon, winter, Gulf of Alaska, pathogens, stressors

Introduction

The semelparous and anadromous life history of Pacific salmon (*Oncorhynchus* spp.) makes them crucial to coastal and terrestrial ecosystems around the North Pacific by connecting oceanic and terrestrial food webs and nutrient cycles (Cederholm et al. 1999; Radchenko 2006). Similarly, salmon are highly valued around the northern Pacific Rim due to their significant contribution to commercial and recreational fisheries as well as their cultural importance, especially for Indigenous Peoples (Lichatowich and Lichatowich 2001). Despite this significance, many wild Pacific salmon stocks have experienced population fluctuations and declines throughout their range, most notably on their southern distribution limits, due to a combination of compounding factors. Most prominently featured are overexploitation, habitat degradation, pathogens, predators, prey availability, and climate

change (Rand 2002; Ruckelshaus et al. 2003; Miller et al. 2014). A vivid display of these influences is the long-term fluctuation and decline of sockeye salmon returns to the Fraser River in British Columbia, Canada, which in 2019 and 2020 reached their lowest levels in recorded history (psc.org/publications/fraser-panel-in-season-information/).

Efforts to rebuild stocks include habitat restoration, stock enhancements through hatcheries, and stock monitoring through several assessment methods intended to inform targeted management strategies (Cooke et al. 2012). These monitoring strategies include spawning escapement and smolt survival assessments as well as test fisheries in riverine and coastal waters (Woodey 1987; Irvine and Akenhead 2013; Zimmerman et al. 2015; Kendall et al. 2017). Recent advances in molecular methods have also allowed the health surveillance of individual salmon through the detection of infectious agents and use of host "biomarker panels" to assess health and condition using a high throughput nanofluidics quantitative polymerase chain reaction (qPCR) approach (Miller et al. 2014, 2016; Houde et al. 2019). While these novel genetic tools have been applied on the coastal margins to identify infection-related factors associated with health and survival of juvenile and adult salmonids, the open ocean remains a key compartment of the life cycle of Pacific salmon where information is virtually absent due to insufficient sampling.

Salmon stocks and species vary considerably in the length of time they spend on the coastal margin after smoltification, but most Pacific salmon ultimately leave coastal waters and head out into the open ocean of the North Pacific. There, they spend one to six years gaining the majority of their body mass feeding on marine resources, but since these remote open-ocean habitats are not under the direct jurisdiction of nations, the factors influencing salmon productivity and survival are poorly understood, despite the observed large temporal shifts in marine survival over recent decades (Holtby et al. 1990; NAGASAWA and K 2000; Radchenko 2012; Naydenko, Temnykh and Figurkin 2016; Shuntov, Temnykh and Naydenko 2019). Pacific salmon stocks mix in the ocean, meaning that fish from home streams as distant as North America and Asia might be found in the same aggregation (Wood, Rutherford and McKinnell 1989; Beacham et al. 2009; Urawa et al. 2009, 2016). The Northwestern and central North Pacific have been the subject of decade-long research efforts of Russian and Japanese researchers and are comparatively well understood, allowing Russian researches to predict returns of pink salmon with unparalleled precision (Startsev and Rassadnikov 1997; Shuntov and Temnykh 2011; Beamish 2018). Comprehensive surveys of the Northeastern Pacific on the other hand remain absent, with only a small number of spatially and temporally limited observations during long-line and drift net operations in the 1960s and 1990s, and a single trawl transect in 2006 (Welch et al. 1995; UENO and Y 1999; Fukuwaka, Sato and Takahashi 2007; Beacham et al. 2009). The winter months in particular, when open-ocean conditions might critically impact ocean survival of first ocean-winter juvenile and subadult salmon, are the least understood but could largely determine stock performance (Ishida et al. 2000; NAGASAWA and K 2000; Beamish and Mahnken 2001; Naydenko et al. 2016; Shuntov et al. 2017). Despite progress on salmon marine ecology during the winter, questions regarding the health and survival of salmon during this period remain unanswered, specifically in the open ocean.

To address these knowledge gaps, we performed an end-of-winter survey in the Gulf of Alaska (GoA) in February and March of 2019. Under the banner of the International Year of the Salmon initiative, scientists from the five member nations of the North Pacific Anadromous Fish commission (NPAFC: Russia, Canada, United States, South Korea, and Japan) collaborated onboard the Russian research trawler *Prof. Kaganovskiy* to conduct oceanographic sampling and trawl surveys to provide the baseline data for future pan basin studies.

Here we present a comprehensive overview on the health and condition of 252 overwintering individuals, including coho, chum, pink, and sockeye salmon, sampled in the GoA. We survey the

prevalence and load of 48 infectious agents—not only well-established or opportunistic salmon pathogens for which Koch's postulates have been demonstrated (Miller et al. 2014), but also several newly discovered viruses with unknown pathogenic potential that are thus referred to as infectious agents (Mordecai et al. 2019, 2020)—by high throughput qPCR. We deploy Fit-Chips, a recently developed genomic technology to recognize specific stressors and disease states in salmon, to assess trends in the expression of 89 genes associated with a wide range of stressors and correlate these two measures of individual health and oceanographic observations. For selected agents, we also verify infection and assess potential for disease through histopathology. Finally, we contrast these findings with observations from the coastal margins and suggest mechanisms that govern infectious-agent burden in the open ocean that might influence marine survival.

Methods

Sampling

Samples of Pacific salmon were collected during the 2019 International Year of the Salmon GoA expedition in February and March 2019 onboard the Russian research trawler *Prof. Kaganovskiy*. Sixty 1 h trawls accompanied by oceanographic sampling were performed along a grid of stations separated by 1 degree of latitude or 1.5 degrees longitude (approximately 110 km apart), and 422 salmon were captured over the course of the expedition (**Supplementary Material, Fig. 1**, **Supplementary Material, Table 1**). Subsampled salmon from all species were dissected in a clean environment within one hour of capture (**Supplementary Material, Fig. 2**). Notes on gross pathologies were collected during dissections. Presence of nematodes in organs or the peritoneum was noted on a nonspecies-specific level; no other macroscopic parasites were observed. Tissue samples were preserved in RNAlater (Thermo Fisher Scientific, MA, USA) for nucleic acid extraction as well as in 10% neutral buffered formalin for histopathology.

Genetic stock identification

Genetic stock identification for coho and sockeye salmon was performed by the Department of Fisheries and Oceans Canada, Pacific Biological Station Molecular Genetics Laboratory as described by Beacham et al. (2010, 2020).

Oceanographic data

Oceanographic data were collected at each station with a 24-position rosette equipped with CTD sensors as described by Pakhomov et al. (2019). Turbidity, fluorescence, and oxygen saturation were measured, and water samples were collected for assessing salinity, chlorophyll, and macronutrients. To survey zooplankton communities two Juday nets as well as one Bongo net were deployed as described by Pakhomov et al. (2019).

Calorimetry

Calorimetric data on the energy content of salmon individuals in this study was provided by the National Oceanic and Atmospheric Administration, Alaska Fisheries Science Center, Auke Bay Laboratories in Juneau, Alaska, USA, for 46 Sockeye. In brief, tissue samples were weighed, dried with their skin on at 135 °C, homogenized, and analyzed using bomb calorimetry (kJ/g dry mass) (Siddon et al. 2013).

Nucleic acid extraction and processing

Tissue samples from gill, heart, kidney, and spleen were homogenized using TRI-reagent (Ambion Inc., Austin, Texas), and 1-bromo-3-chloropropane was added to the homogenate. Total RNA was extracted from the aqueous phase using the Total RNA Isolation kits (Ambion Inc., Austin, Texas)

on a Biomek FXP liquid handling instrument (Beckman-Coulter, Mississauga, Ontario, Canada) (Miller et al. 2011; Jeffries et al. 2014). RNA quality was assessed after DNase treatment by spectrophotometry and RNA was normalized to 62.5 ng/µL so that 1 µg of RNA was used for cDNA synthesis (SuperScript VILO MasterMix, Life Technologies).

DNA was extracted from the organic/interphase of TRI-reagent using a high salt TNES-urea buffer (Asahida et al. 1996) followed by the BioSprint 96 DNA extraction kit (Qiagen, MD). DNA quantity and quality were assessed by spectrophotometry on a Beckman Coulter DTX 880 Multimode Detector (Brea, CA, USA). Samples were normalized to 62.5 ng/µL.

For infectious agent monitoring, cDNA from all pooled organs was mixed with equal amounts of pooled DNA extract from all organs to 1.25 µL final volume. Samples were pre-amplified with primer pairs for all 48 infectious agent assays (Table 1) in a 5 µL reaction using TaqMan PreAmp Master Mix (Life Technologies), following the BioMark protocol, to increase sensitivity of the small assay volume (7 µL) on the dynamic arrays. Unincorporated primers were eliminated using ExoSAP-IT PCR Product Cleanup (MJS BioLynx Inc., Ontario, Canada). Samples were diluted 1:5 in DNA Suspension Buffer (TEKnova, Hollister, California). An assay mix containing 9 µM artificial positive control clones (labelled with fluorescent dye VIC) allowed for the detection of contamination. For host gene expression monitoring, an equivalent procedure was performed on cDNA from gill tissues only, targeting 89 host genes individually. A serial dilution of pooled gill cDNA was used to assess assay efficiency across runs.

High throughput qPCR infectious agent screening

The qPCR assays and individual samples were loaded onto 96.96 dynamic arrays (Fluidigm, San Francisco, CA, USA) and run on the BioMark[TM] HD platform. The same distribution of assays was used for each array and samples from different dates and locations were stratified among arrays. The Fluidigm 2 × Assay Loading Reagent was mixed with primer pairs and probes to 5 µL per well. A 5 µL sample loading mix was prepared using 2 × TaqMan Gene Expression Master Mix (Life Technologies), 20 × Gene Expression Sample Loading Reagent, and 2.7 µL of pre-amplified cDNA. The reaction mixes were added to the assay and sample inlets of the dynamic array as per the manufacturer's protocols and loaded into the chip by an integrated fluidic circuit controller HX (Fluidigm). PCR was performed under the following conditions: 50 °C for 2 min, 95 °C for 10 min, followed by 40 cycles of 95 °C for 15 s and 60 °C for 1 min.

In addition to known pathogens, we incorporated assays for newly discovered putative viruses of unknown pathogenic potential. These viruses originate from an unpublished polyA amplified meta-transcriptomic sequencing library from 20 Chinook salmon targeting unknown infectious agents. We screened these libraries using a translated blast search (see Mordecai et al. 2019 for methods) and found short contigs (Genbank accessions MW373508-MW373514, **Supplementary Material, Table 2**). These contigs showed protein homologies to hanta-like, rhabdo-like, picorna-like, and qin-like viruses, as well as contigs with high sequence homology to an unpublished viral contig SalmovirusWFRC1 (NC_034441). Additionally, we included an assay for a sequence variant of Pacific salmon Nidovirus (PsNV; Mordecai et al. 2020) and a co-infected bafini-like virus (**Supplementary Material, Table 2**).

Infectious agent screen analysis

Cycle threshold (CT) for each assay was determined using the BioMark Real-Time PCR analysis software (Fluidigm). For each infectious agent assay, samples with detection in only one duplicate were treated as negatives and duplicate values were averaged. Samples contaminated by high load controls (indicated by VIC positives) were removed. Amplification curves of all assays were visually assessed

Table 1. Primers and probes utilized in the infectious agents and pathogen screen.

Assay name	Type (strain)	Name	Reference	Primer_F	Primer_R	Probe
ae_sal	Bacterium	*Aeromonas salmonicida*	Miller et al. (2016)	TAAAGCACTGT CTGTTACC	GCTACTTCAC CCTGATTGG	ACATCAGCAGGCTT CAGAGTCACTG
c_b_cys	Bacterium	*Candidatus Branchiomonas cysticola*	Mitchell et al. (2013)	AATACATCGGAAC GTGTCTAGTG	GCCATCAGCC GCTCATGTG	CTCGGTCCCAGGCTT TCCTCTCCCA
pch_sal	Bacterium	*Piscichlamydia salmonis*	Nylund et al. (2008)	TCACCCCCA GGCTGCTT	GAATTCCATTT CCCCCTCTTG	CAAAACTGCTA GACTAGAGT
pisck_sal	Bacterium	*Piscirickettsia salmonis*	Corbeil et al. (2003)	TCTGGGAAGTG TGGCGATAGA	TCCCGACCTACT CTTGTTTCATC	TGATAGCCCCGTACA CGAAACGGCATA
re_sal	Bacterium	*Renibacterium salmoninarum*	Powell et al. (2005)	CAACAGGGTGGT TATTCTGCTTTC	CTATAAGAGC CACCAGCTGCAA	CTCCAGCGCCG CAGGAGGAC
rlo	Bacterium	Rickettsia-like organism (RLO)	Lloyd et al. (2011)	GGCTCAACCC AAGAACTGCTT	GTGCAACAG CGTCAGTGACT	CCCAGATAACCGCC TTCGCCTCCG
sch	Bacterium	*Candidatus Syngnamydia salmonis*	Duesund et al. (2010)	GGGTAGCCCGA TATCTTCAAAGT	CCCATGAGCC GCTCTCTCT	TCCTTCGGG ACCTTAC
te_mar	Bacterium	*Tenacibaculum maritimum*	Miller et al. (2016)	TGCCTTCTACA GAGGGATAGCC	CTATCGTTGCC ATGGTAAGCCG	CACTTTGGAA TGGCATCG
vi_ang	Bacterium	*Vibrio anguillarum*	Miller et al. (2016)	CCGTCATGCTATCT AGAGATGTATTTGA	CCATACGCAGC CAAAAATCA	TCATTTCGACGAG CGTCTTGTTCAGC
vi_sal	Bacterium	*Vibrio salmonicida*	Miller et al. (2016)	GTGTGATGAC CGTTCCATATTT	GCTATTGTCATC ACTCTGTTTCTT	TCGCTTCATGTTGTG TAATTAGGAGCGA
ye_ruc_glnA	Bacterium	*Yersinia ruckeri*	Miller et al. (2016)	TCCAGCACCA AATACGAAGG	ACATGGCAG AACGCAGAT	AAGGCGGTTACTT CCCGGTTCCC
ce_sha	Parasite	*Ceratanova shasta*	Hallett and Bartolomew (2006)	CCAGCTTGAGA TTAGCTCGGTAA	CCCCGGAA CCCGAAAG	CGAGCCAAGTTGGTCT CTCCGTGAAAAC
de_sal	Parasite	*Dermocystidium salmonis*	White et al. (2013)	CAGCCAATCC TTTCGCTTCT	GACGGACGCA CACCACAGT	AAGCGGCGTGTGCC
ic_hof	Parasite	*Ichthyophonus hoferi*	Miller et al. (2016)	ACGAACTTAT GCGAAGGCA	TGAGTATTCAC TYCCGATCCAT	TCCACGACTGCAA ACGATGACG
ic_mul	Parasite	*Ichthyophthirius multifiliis*	Miller et al. (2016)	GTCTGTACTGG TACGGCAGTTTC	TCCCGAACTCAG TAGACACTCAA	TAAGAGCACCCACT GCCTTCGAGAAGA
IcD	Parasite	*Ichthyobodo sp.*	Miller et al. 2016	AAATGGGCAT ACGTTTGCAAA	AACCTGCCTGAAA CACTCTAATTTTT	ACTCGGCCTTCACT GGTTCGACTTGG

(continued)

Table 1. (*continued*)

Assay name	Type (strain)	Name	Reference	Primer_F	Primer_R	Probe
ku_thy	Parasite	*Kudoa thyrsites*	Fukuwaka et al. (2007)	TGGCGGCCA AATCTAGGTT	GACCGCACACA AGAAGTTAATCC	TATCGCGAGAGCCGC
lo_sal	Parasite	*Loma sp.*	Miller et al. (2016)	GGAGTCGCAG CGAAGATAGC	CTTTTCCTCCCTTT ACTCATATGCTT	TGCCTGAAATCACGA GAGTGAGACTACCC
my_arc	Parasite	*Myxobolus arcticus*	Miller et al. (2016)	TGGTAGATACTGA ATATCCGGGTTT	AACTGCGCGG TCAAAGTTG	CGTTGATTGT GAGGTTGG
my_ins	Parasite	*Myxobolus insidiosus*	Miller et al. (2016)	CCAATTTGGG AGCGTCAAA	CGATCGGCAAAG TTATCTAGATTCA	CTCTCAAGGCATTTAT
na_sal	Parasite	*Nanophyetus salmincola*	Miller et al. (2016)	CGATCTGCATTTG GTTCTGTAACA	CCAACGCCACAAT GATAGCTATAC	TGAGGCGTG TTTTATG
ne_per	Parasite	*Neoparamoeba perurans*	Fringuelli et al. (2012)	GTTCTTTCGGG AGCTGGGAG	GAACTATCGCCGG CACAAAG	CAATGCCATTC TTTTCGGA
pa_kab	Parasite	*Parvicapsula kabatai*	Miller et al. (2016)	CGACCATCTGC ACGGTACTG	ACACCACAACT CTGCCTTCCA	CTTCGGGTA GGTCCGG
pa_min	Parasite	*Parvicapsula minibicornis*	Hallett and Bartolomew (2009)	AATAGTTGTTTGTC GTGCACTCTGT	CCGATAGGCTATCCA GTACCTAGTAAG	TGTCCACCTA GTAAGGC
pa_pse	Parasite	*Parvicapsula pseudobranchicola*	Jørgensen et al. (2011)	CAGCTCCAGTA GTGTATTTCA	TTGAGCACTCTGC TTTATTCAA	CGTATTGCTGTCT TTGACATGCAGT
pa_ther	Parasite	*Paranucleospora theridion/Desmozoon lepeophtherii*	Nylund et al. (2010)	CGGACAGGGA GCATGGTATAG	GGTCCAGGTT GGGTCTTGAG	TTGGCGAAG AATGAAA
sp_des	Parasite	*Sphaerothecum destruens*	Miller et al. (2016)	GGGTATCCTTC CTCTCGAAATTG	CCCAAACTCG ACGCACACT	CGTGTGCGCTTAAT
te_bry	Parasite	*Tetracapsuloides bryosalmonae*	Bettge et al. (2009)	GCGAGATTTGT TGCATTTAAAAAG	GCACATGCAGTG TCCAATCG	CAAAATTGTGGAAC CGTCCGACTACGA
arena1	Virus (SPAV-1)	Salmon pescarenavirus-1	Mordecai et al. (2019)	CCTGCCTCTTT GCTCATTGTG	AGAAAAGCTGTG GTACTTTAGAAAGC	ATCCGCCTA ACGGTTGG
arena2	Virus (SPAV-2)	Salmon pescarenavirus-2	Mordecai et al. (2019)	AACATGAAGGGC GATTCGTT	CAGCCCGCGGACTGAGT	CAAGTGATGT AAGCTTG
Bafini_b	Virus	Putative bafini virus	This study	TCAATAAGGGC CAGCGACAT	CCATTGCTTATC AGGCTCTTCA	CTGTGACAT GATTTTC
Circo	Virus	Putative circo virus	This study	AAGCCCTCGA TGCCTACGTA	ATGGCCTCTTT CCGACTTCA	AAAAAAGAGA CGAGGATCG

(*continued*)

Table 1. (*concluded*)

Assay name	Type (strain)	Name	Reference	Primer_F	Primer_R	Probe
cov	Virus (PsNV)	Pacific salmon nidovirus	Mordecai et al. (2019)	GGATAATCCCAA CCGAAAAGTTT	GCATGAAATGTT GTCTCGGTTTAA	CGATCCC GATTATC
ctv	Virus (CTV-2)	Cutthroat Trout Virus-2	Mordecai et al. (2020)	CCACTTGTCGCT ACGATGAAAC	CGCCTCCTTT GCCTTTCTC	ATGCCGGGCCATC
Hantavirus	Virus	Putative hantavirus	This study	ATTGCATTCAC CGCAACAAG	GTCCAGCTTTG CCGTTGTCT	CAGGACCAAG AGGTGTT
Nido2_a	Virus	Pacific salmon nidovirus sequence variant	This study	TCAACACCCCC GAAAGAAAC	AAGGAACTGGAGCT TCAGGTAGAG	TACATTTTTGTAG GAACACTACC
ortho	Virus (RbtOV)	Rainbow trout orthomyxovirus	Batts et al. (2017)	GGAAGCAGTGG ACGCTAACC	TCGCGAAGGTCT CTCAATGTC	ATTCTTCTCAT CAAAGGCA
Picorna2	Virus	Putative -picorna virus	This study	GGGAATACTAGC GCTCCTTCCT	TGGACCGACCAT GAAGAAGAA	CTCTATGAGG CGGCAGG
prv	Virus (PRV-1)	Piscine orthoreovirus-1	Garseth et al. 2013	TGCTAACACTCCA GGAGTCATTG	TGAATCCGCTGC AGATGAGTA	CGCCGGTAGCTCT
pspv	Virus	Pacific salmon parvovirus	Nekouei et al. (2018)	CCCTCAGGCTCC GATTTTTAT	CGAAGACAACAT GGAGGTGACA	CAATTGGAGG CAACTGTA
Qin	Virus	Putative Qin-like virus	This study	TCACCTCACGCT CAGAAAGCT	GCGAAGTCATAG CCTTCAACGT	TTCTCAAGTGTT TTGGATGTT
reov	Virus (CAV)	Chinook aquareovirus	Mordecai et al. (2019)	AACTTTCGGCTTT CTGCTATGC	GAGGACAAGGG TCTCCATCTGA	TTAATTGCGG TACTGCTC
Rhabdo3	Virus	Putative rhabdo virus	This study	TGAGCTAGCACTTT CACCACAGTAT	GTTGGAGCATATTG AATCTTTTAGTCA	CCTGACTGC TGATTCT
Salmovirus	Virus	SalmovirusWFRC1	NC_034441	CCGGCCCTG AACCAGTT	GTAGCCAAGTGG GAGAAAGCT	TCGAAGTG GTGGCCAG
smallUK	Virus (PRNAV)	Putative RNA virus	Mordecai et al. (2020)	GTACCTAATTTAACT GGAACAGTAGAC	CGTTCAGTAACAC AAGTATCCAAA	TGCAACAGGCAAGT GATATGCTTGA
ven	Virus (ENV)	Erythrocytic necrosis virus	J. Winton, pers. Comm.	CGTAGGGCCC CAATAGTTTCT	GGAGGAAATGCA GACAAGATTTG	TCTTGCCGTTATTT CCAGCACCCG
ver	Virus	Viral encephalopathy and retinopathy virus	Korsnes et al. (2005)	TTCCAGCGAT ACGCTGTTGA	CACCGCCCGTGTTTGC	AAATTCAGCCAA TGTGCCCC
vhsv	Virus	Viral hemorrhagic septicemia virus	Jonstrup et al. 2013	AAACTCGCAGGA TGTGTGCGTCC	TCTGCGATCTCA GTCAGGATGAA	TAGAGGGCCTTGGT GATCTTCTG

Table 2. Primers and probes utilized in the Fit-Chip biomarker gene expression survey.

Gene	Panel 1 (Panel 2; Panel 3)	Gene Name	Primer_F	Primer_R	Probe
AARDC	ImMort	Arrestin domain containing 2	AAGAAAGCCAAGGCGTGAGTAA	TCGGTTGCCAGGGTTAGC	TGGAGGACAAATCGGA
ATP5G3	MorRel	ATP synthase lipid-binding protein, mitochondrial precursor	GGAACGCCACCATGAGACA	CGCCATCCTGGGCTTTG	AGCCCCATTGCCTC
AURKB	Hypox (ImMor)t	Aurora kinase B-like	GAAATGTGGTCGCTTCGATGA	CATCAGCCAACTCCTCCATGT	CAGCGCACTGCTAC
B2M	ImmStim	B2M	TTTACAGCGCGGTGGAGTC	TGCCAGGGTTACGGCTGTAC	AAAGAATCTCCCCCCAAGGTGCAGG
BSG	ImMort	Basigin	CGTGGCCGAGGTCATCAT	TCAGGCTTTCTCCTCTTCTCGTA	TGGTCAGCATCATCTT
C7	MorRel	Complement component C7 precursor	GATGCTGACCACATCAAACTGC	ACCTCTGTCCAGCTCTGTGTC	AACTACCAGACAGTGCTG
VAR1	VDD	VAR1	CCACCTGAGGTACTGAAGATAAGACA	TTAAGTCCTCCTTCCTCATCTGGTA	TCTACCAGGCCTTAAAG
2-Mar	MorRel	E3 ubiquitin-protein ligase MARCH2	GCACCTGCGATAGAAGAGCAT	GAGATGGAATCCGCAGAAGCT	ACTTGTTTAACCATGCTGTGCGACTCTCCT
CBEBP	GenStr (ImMor)t	CCAAT/enhancer binding protein (C/EBP), beta	AACTGGCCGCAGAGAATGAC	AAGTTACGCAGAGTGGCAAGCT	TTTACAAAAACGCGTGGAGC
CD83	ImmStim	CD83	GTGGCGGCATTGCTGATATT	CTTGTGGATACTTCTTACTCCTTTGCA	CACCATCAGCTATGTCATCC
CDKN1B	ImMort (Hypox)	Cyclin dependent kinase inhibitor 1B	CGTCCTCAGCGAAATGGAA	CCATTCGAATCTCCCGTTTAAT	TCGATTTTTCAAGTCAAAC
CFTR_1	GenStr	Cystic fibrosis transmembrane conductance regulator I	ACGCCTGTCCAAAGATAGTGTCTA	GCAAAGCATTGCTCCATATCC	AGCGAGGATGTGGACG
CIT	Hypox	Citron Rho-interacting kinase-like	GATCTCTAGGTTTCAGCGCAAGA	TGAGCTCCACATCCTTTTGGT	ACCTGGAGTCAGTTCT
CLASPIN	Hypox	Claspin-like	ATGCGGGCTGCCCTATC	CTCTTGAAGAACTGGTCGATGCT	CATGCCTGAGCCCAA
CLEC4E	ImMort	C-type lectin domain family 4, member E	CCTGAGGGCTGGATTCATGT	TCGGCCAGTCCATCTTGTC	TGAGAAATGTTACTCCTTCAGT
COX6B	Hypox	Cytochrome C oxidase	GCCCGTGTGACTGGTATAAG	TCGTCCCATTTCTGGATCCA	TCTACAAATCACTGTGCCC

(*continued*)

Table 2. (*continued*)

Gene	Panel 1 (Panel 2; Panel 3)	Gene Name	Primer_F	Primer_R	Probe
DEXH	VDD	ATP-dependent RNA helicase	CCATAAGGAGGGTGTCTACAATAAGAT	CTCTCCCCCTTCAGCTTCTGT	TGGCGCGCTACGTG
EF2_1	TherStr	Elongation factor 2	GGAATTTAGTGGATGTCTGACCATT	TCCCATCCCTCACTCGTACAG	CCCATTCCTTCTATTCCT
EF2_2	TherStr	Elongation factor 2	AGGTCACAGCCGCCCTTAG	ACACAGTCTCTGTCTGCACACACA	CGACTGCGTCTCAGGT
EPD	Infl	Ependymin	ACAAGACATTCGGCCTGGAT	CGGTTCTTGTGGTTAATCGTATACA	CCCTTCTGCTCTTCA
ERCC6L	Hypox	ERCC excision repair 6-like, spindle assembly checkpoint helicase	TTGTATGGTCTCCACAGAGATGGT	GTCTTCCCTAAGCCCATGTCAT	TCAAGGAGGAATCCTAG
ES1	Infl	ES1 protein homolog	CGGCAACTTCCATGAAGGA	GGACCTCCCCCACTTTCTTATT	TGGGCTGTAAACACG
FKBP10_1	TherStr	FK506-binding protein 10 precursor	ACTATGAGAATGCCCCCATCAC	CTCGTCCAGACCCTCAATCAC	CCTGGGAGCCAACAA
FKBP10_2	TherStr	FK506-binding protein 10 precursor	CCTGAAGAGATCATTGCTGACATG	GACGATGACCCCATCCTTGT	TCAGGAACCAGGACCG
FKBP5	GenStr (ImMort)	FK506-binding protein 5	GGGCGTTCCTCTGGGTGTA	GCATGCAGCATTCTCCTTTCT	ACAGGGCCATGGAGA
FYNTBP	MorRel	FYN-T-binding protein	TGCAGATGAGCTTGTTGTCTACAG	GCAGTAAAGATCTGCCGTTGAGA	CTCAACGATGACATCCACAGTCTCCCC
GAL3	VDD	Galectin-3-binding protein precursor	TTGTAGCGCCTGTTGTAATCATATC	TACACTGCTGAGGCCATGGA	CTTGGCGTGGTGGC
GILT	Infl	Gamma-interferon-inducible lysosomal thiol reductase (GILT)	CTGGTGCCCTATGGAAATGC	CCGTGCTGGCAGGTGAAC	ATCTTTTGATGGGAAGAAG
GLUL	ImMort	Glutamate-ammonia ligase (glutamine synthetase)	GTTCCAGGTTGGCCCTTGT	CCTAGCTGCCCAAAGGTGATC	AAGGCATCAGCATGGG
GPX3	Hypox (ImMor)t	Gutathione peroxidase 3-like	AGGCCAGTCCTTCAGTGCAT	GGCAGGACCAGGAGGTAACA	TGGGCCTGGTAACC
H2EB1	ImMort (ClLev)	Histocompatibility 2, class II antigen E beta	CAGTTGAGCCCCATGTCAGA	TCAGCATGGCAGGGTGTCT	TGAGCTCAGTGACTCC
HEP	ImmStim	Hepcidin	GAGGAGGTTGGAAGCATTGA	TGACGCTTGAACCTGAAATG	AGTCCAGTTGGGGAACATCAACAG

Table 2. (*continued*)

Gene	Panel 1 (Panel 2; Panel 3)	Gene Name	Primer_F	Primer_R	Probe
HERC6	VDD	Probable E3 ubiquitin-protein ligase HERC6	AGGGACAACTTGGTA GACAGAAGAA	TGACGCACACACA GCTACAGAGT	CAGTGGTCTCTG TGGCT
HLA2G	ImMort (ClLev)	HLA class 2 gamma	CCAGGACGTTATC CTCCCAAT	GAGAAGACACGCC AGCACTGT	AGGGCCTC TAACAGC
HSC70	ImMort (OsStr; GenStr)	Heat shock cognate 70 kDa protein	GGGTCACACAGAA GCCAAAAG	GCGCTCTATAGC GTTGATTGGT	AGACCAAGCCTAAACTA
HSP70	TherStr	Heat shock 70 kDa protein	TCAACGATCAGG TCGTGCAA	CGTCGCTGACCA CCTTGAA	CCGACATGAAGCACTGG
HSP90al	TherStr	Heat shock proteina 90 alpha-like	TTGGATGACCC TCAGACACACT	CGTCAATACCCAG GCCTAGCT	CCGAATCTACCGGATGAT
HSP90	GenStr	Heat shock protein 90	TGGGCTACATGG CTGCCAAG	TCCAAGGTGAAC CCAGAGGAC	AGCACCTGGAGATCAA
HSP90a	ImMort (GenStr; OsStr)	Heat shock protein 90 alpha	ATGACCCTCAGAC ACACTCCAA	CCTCATCAATACCC AGTCCTAGCT	CGCATCTACAGAATGA
HTATIP	MorRel	HIV-1 Tat interactive protein	CTTGTAACAGTTCG ACATGGCTTATT	TGGTGAAGCATTTC TGTATGTCAA	TCTGTACTGAGCATCCCC GCACATTACA
ICLP2	ImMort (ClLev)	Invariant chain-like protein 2	CAGCAGAAGGGTCC AACAAGAG	TCCTGCAGGTCTT TAATGTCGTT	TTCAAGATAGCTG GTTTCAC
IFI	VDD	IFN-induced protein	GCTAGTGCTCTTGAG TATCTCCACAA	TCACCAGTAACTCTG TATCATCCTGTCT	AGCTGAAAGCACTTGAG
IFI44	VDD	IFN-induced protein 44-1	CCACTGGACT AACCCTCCATGA	TGTGTCCCTCG GGTGCAT	ACTCTGGCTATCATCAAA
IFIT5	VDD	Interferon-induced protein with tetratricopeptide repeats 5	CCGTCAATGAGT CCCTACACATT	CACAGGCCAATTT GGTGATG	CTGTCTCCAAACTCCCA
IFNa	ImmStim	IFN-alpha	CGTCATCTGCA AAGATTGGA	GGGCGTAGCTTC TGAAATGA	TGCAGCACAGATGTAC TGATCATCCA
IGMs	ImmStim	IgM (sec.) AB044939	CTTGGCTTGTT GACGATGAG	GGCTAGTGGTGTT GAATTGG	TGGAGAGAACGAG CAGTTCAGCA
IL_11	Infl	Interleukin11	GCAATCTCTTGC CTCCACTC	TTGTCACGTGCT CCAGTTTC	TCGCGGAGTGTG AAAGGCAGA
IL_15	ImmStim	Interleukin15	TTGGATTTTGCC CTAACTGC	CTGCGCTCCAAT AAACGAAT	CGAACAACGCTG ATGACAGGTTTTT

(*continued*)

Table 2. (*continued*)

Gene	Panel 1 (Panel 2; Panel 3)	Gene Name	Primer_F	Primer_R	Probe
IL_17D	Infl	Interleukin17D NM 001124399	CAACAGAAGTGC GAACGATG	GATGCCACATCGC ATAACAG	TGGTCGAGTATCTTTC GTGTGTTTGC
IL_1b	ImmStim	Interleukin1 beta	AGGACAAGGACCT GCTCAACT	CCGACTCCAACTC CAACACTA	TTGCTGGAGAGT GCTGTGGAAGAA
IQGAP1	ImMort	IQ motif containing GTPase activating protein 1	GAGGGTGTGGCT GTGATGAA	CAGGAAGATGAGC AGGTTGACA	CTCTTCGACAGGGCC
IRF_1	MorRel	Interferon regulatory factor 1 (IRF-1) gene	CAAACCGCAAGAG TTCCTCATT	AGTTTGGTTGTGTTT TTGCATGTAG	CTGGCGCAGCAGATA
JUN_F3	GenStr	7_4_4_6_Transcription factor AP-1	TTGTTGCTGGTGAGA AAACTCAGT	CCTGTTGCCCTATG AATTGTCTAGT	AGACTTGGGCTATTTAC
KIF15	Hypox	Kinesin family member 15	CAGGCAGGTCTTCTC CAAGCT	AGTTTGGATGATAGCC TCCTTCTG	CACAGGATCAGACTGC
KIF2C	Hypox	Kinesin-like protein KIF2C	CGGCCAAACTGGAA GTGGTA	TTCTGGCTCTTCCC TGAAAAGT	AACTCACACAATGGGAG
KRT8	MorRel	Cyclokeratin-8	CGATTGAGCGGC TGGATAA	GCATTGTTTACCTTTG ACTTGAATTG	CCCCCTTCTCTACTCTC TTGCTCACCATTC
LDHba	ImMort (GenStr)	L-lactate dehydrogenase B-A chain-like	GTCACTGCTCCCATT TTACACTCTAG	CCCAAACTCCCTCCCA GATAAC	CTGTTCTTAGCTTCCC
Map3k14	TherStr	Mitogen-activated protein kinase kinase kinase 14	GCTCCCTGGGTT CATGGAT	GCCTCCCTTCAGCA GAGACA	CCAGCAATAGCTTATG
MFHAS1	Hypox	Malignant fibrous histiocytoma-amplified sequence 1 homolog	CCGAGGCCTGG GTGAAC	TCAGCTGCTCCACA GAGAAGAA	TCAGTGGCTGCTAGTC
MHC_IIb	ImmStim	MHCII b chain	TGCCATGCTGA TGTGCAG	GTCCCTCAGCCA GGTCACT	CGCCTATGACTTCTAC CCCAAACAAAT
MMP13	Infl	Matrix metalloproteinase-13	GCCAGCGGAGCAGGAA	AGTCACCTGGAGG CCAAAGA	TCAGCGAGATGCAAAG
MMP25	Infl	Matrix metalloproteinase-25 precursor	TGCAGTCTTTTCC CCTTGGAT	TCCACATGTACCCA CACCTACAC	AGGATTGGCTGGAAGGT
MX	VDD	Mx	AGATGATGCTGCAC CTCAAGTC	CTGCAGCTGGGA AGCAAAC	ATTCCCATGGTGATC CGCTACCTGG
NAPEPLD2	Infl	N-acyl-phosphatidylethanolamine-hydrolyzing phospholipase D	CAGACACTCCCTG GCTATTCACT	CCTGAGTCTCACTG GAGGCTCTA	AACCTTCGCTTTA GCTTACGA

Table 2. (*continued*)

Gene	Panel 1 (Panel 2; Panel 3)	Gene Name	Primer_F	Primer_R	Probe
NUPR1	ImMort	Nuclear protein 1	GGAAGCCAGCGA CAATACCA	GGGTTAGCCGTC CGATTTG	CACGAGCGCAAGCT
ODC1	ImMort	Ornithine decarboxylase 1	CCAGAAGGCTC CCTGTTTCA	GCAGCCATTTCCT GGAGAAG	ACAACCCAATCTCA
P_RAS	MorRel	Oncorhynchus mykiss G-protein (P-ras) mRNA, complete cds	GCAGGATGAGCAGA GGAAGAA	GGCCTGGGCAAT GTAACACT	CCCCCTAAAGATGCAG
PRLR	OsStr	Prolactin receptor	GATGCCGGAGGGA AAAGAC	CCGACTGGCTCT TGGACTTG	TCCAAGATGTTGGCTGC
PSMB7	ClLev	Proteasome (prosome, macropain) subunit, beta type 7	AGGAACCCACGTG TCGTGAT	TGGCCCCGGTACC TGAATA	CAGTAAACATATTA CAGGACATG
PSMB8	ImMort (ClLev)	Proteasome (prosome, macropain) subunit, beta type 8	CTGGTTGTGGTAGCA GCTATGC	CGCCTCCTCTACC GTCATGT	TACGGAGTGATGG ACAGC
RAMP1	Hypox	Receptor activity-modifying protein 1-like	CGAACCAAGTGGTG CAAGACT	CCGGACATGCC TGGAAGA	CTTCATCCAG ATCCATTC
RGS21	GenStr	Regulation of G protein signalling 21	TCCCGACTACAGC GCAGAT	TCCTCAGGGCTA AGTCGTTCA	TTCCCAATCCCCC
RIG1	ImmStim	Retinoic acid-inducible gene I	ACAGCTGTTACACAG ACGACATCA	TTTAGGGTGAG GTTCTGTCCGA	TCGTGTTGGACCCCA CTCTGTTCTCTC
RPL6	MorRel	Neoplasm-related protein C140	CGCCACCACAA CCAAGGT	TCCTCAGCCTCTTC TTCTTGAAG	AGATCCCCAAGACTC TGTCAGACGCCT
RRl	Hypox	Ribonucleoside-diphosphate reductase large subunit-like	GCTGGAAGCAGG GTCTGAAG	GTTGGCTGCAG GCTTGGT	CGGGCATGTACTACCT
RRM2	Hypox	Ribonucleoside-diphosphate reductase subunit M2-like	TGCTGCTAGTGAT GGCATTGT	TTTGGAAACCATAG AAGCATCTTG	ATTTACACAGGAA GTCCAGG
RSAD2	VDD	Radical S-adenosyl methionine domaine-containing 2	GGGAAATTAGTCCA ATACTGCAAAC	GCCATTGCTGACA ATACTGACACT	CGACCTCCAGCTCC
SAA	ImmStim	Serum amyloid protein a (SAA)	GGGAGATGATTCAG GGTTCCA	TTACGTCCCCAG TGGTTAGC	TCGAGGACACG AGGACTCAGCA
SCG2	MorRel	Secretogranin2	GGATGTGAAGAATCC AACACTGAT	ACACCACTTCAAACT AGCCATACATT	CGGCTGTATGTG CACTG
SERPIN_1	TherStr	Serpin H1 precursor (HSP47)	ACTATGACCACTCGA AGATCAACCT	CCCATTCGTTGAT GGAGTTCA	AGGGACAAGAGGAGC

Table 2. (*concluded*)

Gene	Panel 1 (Panel 2; Panel 3)	Gene Name	Primer_F	Primer_R	Probe
SERPIN_2	TherStr	Serpin H1 precursor (HSP47)	GAGGTCAGCGACCC AAAGAC	GCCGTAGAGGCGG TTACTGAT	CGGAACGTCACATGGA
SFRS9	TherStr	Splicing factor, arginine/serine-rich 9	ACATTCGTGTCCA CGGAGAAC	GGACCCTCTGCTTT TGTAAGGA	TGCCAGTTATGGTCGCT
SHOP21	GenStr	Hyperosmotic protein 21 (Shop21)	GCGGTAGTGGA GTCAGTTGGA	GCTGCTGACGT CTCACATCAC	CCTGTTGATGCTCAAGG
TAGLN3	ImMort	Transgelin 3	TGGCTCAAGGA CGGATGTG	GGATCTTCCTG ATGGGCTTGT	TGTGTGAACTG ATCAACAG
TGFb	Infl	Transforming growth factor β	TGAGCTCCGTC TCCTCATCA	GCGATTGGCC CATTCCTT	AGAGGCTGGAAC TCTACAG
TRIM1	VDD	Fish virus induced TRIM-1	CATGATGTCTGGTGT TGATGTATATTG	GAGACAGAGAACCA ACTGAGAAAACATA	TTGTCATTCAGAA CCATTG
TXN	Infl	Thioredoxin (txn)	CAAGAATGTGGTT TTCCTCAAGGT	GCATTTGATGTCA CAGTGTTTGG	TGGACGAGGCAGCG
VEGFa	ImMort (GenStr)	Vascular endothelial growth factor A	GGTCTGCTGTGGATA TGAGTATCTTAAA	CCGTTGCACCTC TCAGTGAA	AGCGAAATTGTGA CCATAA
IGF	Growth	Growth cytokine	GACACGCTGC AGTTTGTGTGT	GTGACCGTCGTG AACTGGG	GAGAGAGGCTTTTATTTC AGTAAACCAACGGGG
78 d	Ref	S100 calcium binding protein	GTCAAGACTGG AGGCTCAGAG	GATCAAGCCCCAGA AGTGTTTG	AAGGTGATTCCC TCGCCGTCCGA
Coil	Ref	Coiled-coil domain-containing protein 84	GCTCATTTGAGGAGA AGGAGGATG	CTGGCGATGCTG TTCCTGAG	TTATCAAGCAGCAAGCC
MrpL	Ref	39S ribosomal protein L40, mitochondrial precursor	CCCAGTATGAGGCA CCTGAAGG	GTTAATGCTGCCAC CCTCTCAC	ACAACAACATCACCA

Note: Biomarker panel abbreviations: ImMort, imminent mortality; Hypox, hypoxia; ImmSt, immune stimulation; VDD, viral disease development; MorRel, mortality-related signature; GenStr, general stress; TherStr, thermal stress; Infl, inflammation; ClLev, Cl levels; OsStr, osmotic stress; Growth, growth hormone expression.

for irregularities and consistency between replicates. R statistical software (R Core Team 2017) was used to calculate the efficiencies for each assay using the slope of a regression between CT values and serial dilutions of the artificial positive control standards. We removed values that were not within the linear relationship, often either the lowest or highest RNA concentrations, to improve accuracy of assay efficiency estimates and r^2 values. Only assays with an amplification factor of 1.80–2.20, an r^2 value of ≥0.98, and with typical shaped amplification curves were used in analyses (Larionov et al. 2005). Minimum averaged CT values indicating infectious agent detection with high statistical certainty for each specific infectious agent assay (95% confidence limit of detection), were defined by Miller et al. (2016). Infectious agent prevalence was calculated as the percentage of individuals testing positive for a given infectious agent. All infectious agents found within one host were summarized as a single variable termed "Relative Infection Burden" that takes into account the infection load of all detected pathogens in an individual compared with the population average (Bass et al. 2019). Infectious agent load is the number of copies of a given infectious agent in an individual testing positive. To examine differences between high-sea samples and coastal populations we compared the GoA data with baseline data from coastal British Columbia based on 11 790 wild or nonhatchery marked salmon of all species and age classes sampled between 2014 and 2019 between the Juan de Fuca Strait in the south and waters at the Alaskan border near Dixon Entrance. We calculated location (coast vs GoA) and species-specific relative infection burden (RIB) and Shannon Weaver diversity of infectious agents and compared prevalence of specific agents on a species-specific level using Fisher's exact test (Clarke and Warwick 2001).

Fit-Chip screen of stressors

To determine the primary stressors experienced by salmon in the GoA, we deployed salmon Fit-Chips that utilize curated panels of 89 host genes (biomarkers) to detect transcriptional responses to stressors in gill tissue on the same nanofluidics qPCR platform described above (Miller et al. 2011, 2017; Akbarzadeh et al. 2018; Houde, Akbarzadeh, et al. 2019; Houde, Günther, et al. 2019). Physiological states are recognized based on co-expression of curated biomarker panels that have consistently segregated stress and disease states in challenge studies. For the GoA samples, we applied biomarker panels for hypoxic stress, thermal stress, osmotic stress, general stress, and viral disease development (genes expressed in response to active viral infection), as well as imminent mortality (over-expressed in salmon experiencing mortality within 72 h) and mortality-related (associated with poor long-term survival) markers (Miller et al. 2011, 2017; Akbarzadeh et al. 2018; Houde et al. 2019; Houde et al. 2019). We also included biomarkers associated with different branches of immune stimulation (over-expressed in diseased individuals with known pathogens) and with inflammation (individuals showing pathological signs of inflammation; Table 2). All biomarkers have been assessed for efficiency of amplification across all salmon species, but development of the panels used Chinook and sockeye. Applications across four salmonid species herein offers our first glimpse into recurring patterns of stress- and disease-related gene expression patterns across species co-inhabiting offshore waters of the North Pacific.

Host genes assays were run singularly on cDNA from gill tissues and included three reference genes for normalization (Miller et al. 2016; Teffer et al. 2017). Host gene assay efficiencies were calculated using the serial dilution of pooled pre-amplified host cDNA run on each dynamic array (Miller et al. 2016). Expression heatmaps were visually assessed for failed assays or samples, samples with low expression of reference genes were removed, and failed assays were assigned the mean of the respective species. Samples with less than 55 ng/μL cDNA were excluded from the analysis. Salmon gene CTs were normalized between runs one species at a time using calibrator samples, converted to relative expression by normalizing against the average of the best two out of three reference genes as determined by normfinder, and the relative fold gene expression was calculated using the ddCT

method (Livak and Schmittgen 2001; Jensen and Ørntoft 2004). Assays that failed in more than 50% of individuals for the respective species were excluded from analysis.

Fit-Chip analysis

To gain an overview of gene expression and cluster individuals into groups, expression profiles were visualized as heatmaps using the package ComplexHeatmap in R (Gu et al. 2016). Heatmaps were augmented with pathogen and significantly co-varied metadata between gene expression clusters as determined by analysis of variance (ANOVA) and *t*-test analysis in R (base, stats). To determine the dominant stressors experienced at a population level, we compared the expression of all genes in all individuals of a given species using principal component analysis (PCA). For multidimensional data, PCA identifies the dominant axes (or dimensions) of variation, allowing quantitative interpretation of differential expression among individuals through "ordination" at reduced dimensionality. We deployed the prcomp function in R (base, stats). For visualization, we depict all individuals in the first four dimensions of the PCA, as well as showing the top 20% of genes responsible for ordination in the depicted dimensions as determined by the ordiselect function of the package goeveg in R (cran.r-project.org/web/packages/goeveg/). Three outlier individuals that had dissection comments suggesting severe damage during capture explaining the aberrant gene expression profiles were excluded from the analysis. To interrogate correlations of gene expression with infectious agent, physical, and oceanographic data at site of capture, this information was ordinated onto the PCA plots using the envfit function of the vegan package in R (cran.r-project.org/web/packages/vegan/index.html; Table 3). This function scores correlation of data with the given ordination dimensions and provides a quantitative directional vector depicting this correlation. For visualization, only significant vectors with $p < 0.05$ after 999 permutations are displayed with the metadata name indicating the tip of the scaled arrow segments (Supplementary Figures). We summarized the vectors of all genes belonging to a specific biomarker, and we evaluated the correlation of this superimposed data with the genes driving the ordination using ordiselect in R and the top 20% of genes showing significant correlation in expression with the data (see figures in Results section).

In addition to PCA ordination of gene expression, we also deployed nonmetric multidimensional scaling (NMDS) to describe the different pathogen profiles carried by individuals using the metaMDS function of the vegan package in R. This ordination approach is preferable to PCA for the pathogen data, as it produces an ordination based on abundance rank order, rather than absolute values, which is better able to deal with missing data (in this case absence of pathogen detections). To find the correlations of pathogen profiles with gene expression, physical, and oceanographic data, we used the same approach as described for PCA data above (Table 3).

Results

Salmon infectious agents in the GoA show species-specific trends and lower prevalence than in coastal waters

Infectious agent burden in the GoA is species dependent

All 252 salmon, consisting of 84 chum, 80 coho, 61 sockeye, and 27 pink salmon, were screened by qPCR for 48 microscopic infectious agents commonly observed in British Columbia coastal waters using high throughput qPCR (Table 1). Across all species surveyed, coho had the highest average number of infectious agents detected (3.13), followed by sockeye (2.48), chum (1.86), and pink salmon (1.89) (Supplementary Material, Fig. 3). Similarly, Shannon Weaver infectious agent diversity was highest in sockeye (0.32), followed by coho (0.27), chum (0.18), and pink salmon (0.11; Supplementary Material, Fig. 3).

**Table 3.** Data queried for correlation with gene expression and pathogen profiles.

Metric	Abbreviation	Source	Data generated	Comment
Mass	Mass	This study	Measured	Dissection comment
Fork length	FL	This study	Measured	Dissection comment
Fulton's body condition factor K	K	This study	Calculated	Dissection comment
Sex	Sex	This study	Observation	Dissection comment
Hatchery/wild origin	H/W	This study	Observation	Dissection comment
Presence of wounds and marks	Wound	This study	Observation	Dissection comment
Nematodes	Nematodes	This study	Observation	Dissection comment
Sea lice	Sea_lice	This study	Observation	Dissection comment
Enlarged gallbladder	Gall_bladder	This study	Observation	Dissection comment
Stock and region of origin	Stock	Provided by Fisheries and Oceans Canada, Pacific Biological Station	Genetic stock identification	Only coho and sockeye
Energy density	Cal	Provided by NOAA ABL	Calorimetry	N.A.
Infectious agent load	N.A.	This study	Calculated	See Table 1
Gene expression level	N.A.	This study	Measured	See Table 2
Number of infectious agents detected	number_of_agents	This study	Calculated	N.A.
Relative infection urden	RIB	This study	Calculated	N.A.
Pteropod biomass	Ptero	Pakhomov et al. (2019)	Juday Net	N.A.
Euphausiid biomass	Euphaus	Pakhomov et al. 2019	Juday Net	N.A.
Hydromedusae biomass	Medu	Pakhomov et al. (2019)	Juday Net	N.A.
Caetognats biomass	Caeto	Pakhomov et al. 2019	Juday Net	N.A.
Zooplankton biomass	Zoo_S/M/L	Pakhomov et al. (2019)	Juday Net	N.A.
Temperature	TEM	Pakhomov et al. 2019	CTD	Average of top 100 m
Dissolved oxygen	DO_p	Pakhomov et al. (2019)	CTD	Average of top 100 m
Salinity	SAL	Pakhomov et al. (2019)	CTD	Average of top 100 m
Sea surface temperature	SST	Pakhomov et al. (2019)	Temperature logger on headrope of trawl net	SBE 56 temperature sensor
Latitude	Lat	Pakhomov et al. (2019)	Bridgelog	N.A.
Longitude	Long	Pakhomov et al. (2019)	Bridgelog	N.A.

Note: N.A., not applicable.

Infectious agent profiles in the GoA show species-specific trends

Across all salmon species, 21 of the 48 assayed infectious agents were detected. Two were bacteria, 13 were eukaryotic parasites, and 6 were viruses (Fig. 1; Supplementary Material, Table 3).

Of the two bacterial agents, both opportunistic pathogens, *Candidatus* Branchiomonas cysticola (c_b_cys; assays are listed after the infectious agents, see Table 1 for full list) was detected in all species at high prevalence (56%–89%), whereas *Candidatus* Syngnamydia salmonis (sch) showed modest prevalence in all tested species (4%–11%, Fig. 1; Supplementary Material, Table 3).

FACETS
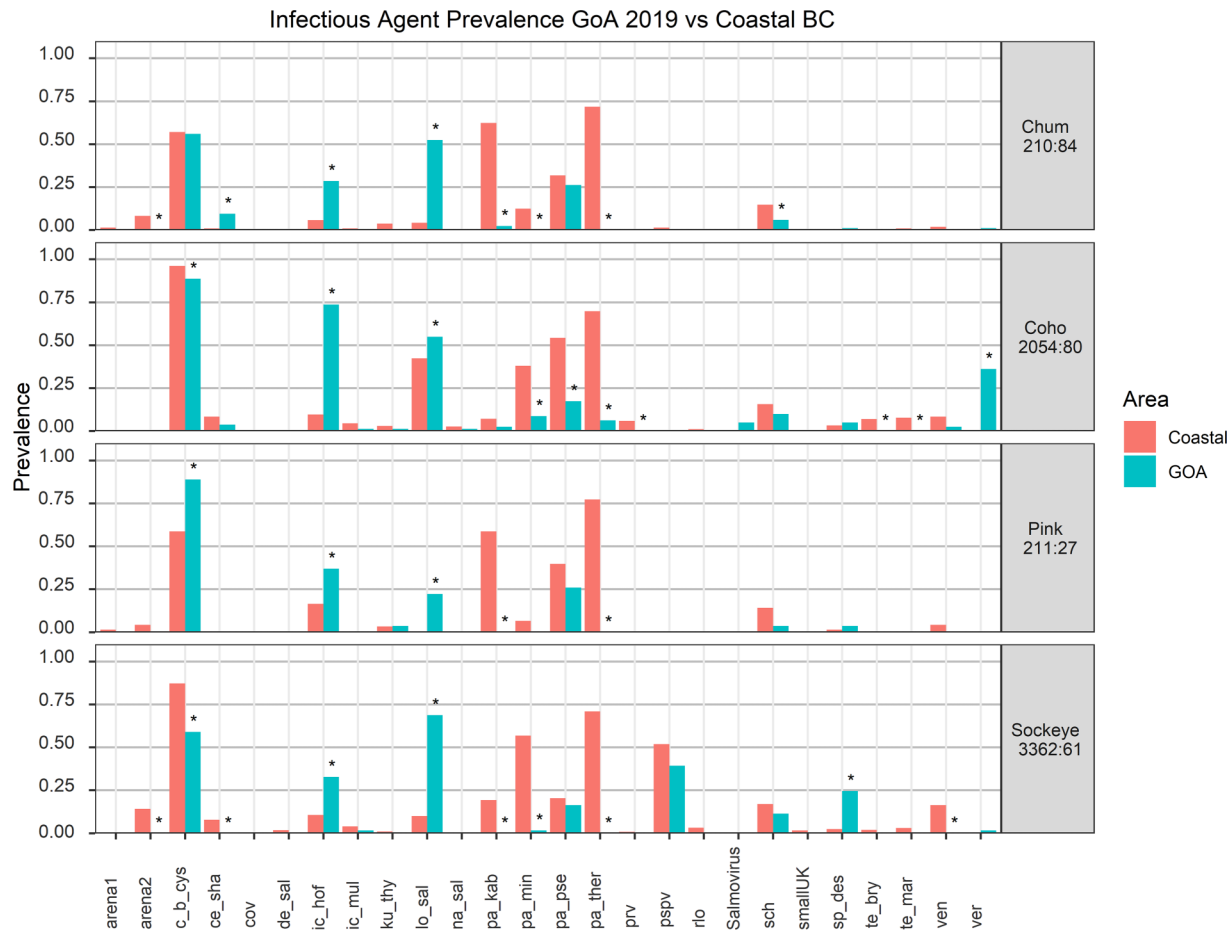
Fig. 1. Comparison of selected infectious agents and pathogens with high prevalence in the Gulf of Alaska (GoA) and Coastal British Columbia. Asterix indicates significant differences in prevalence in the GoA with Fisher's exact test *p* < 0.05. Ratio under species indicates the number of salmon in the analysis for the respective species (coastal:GoA). See **Table 1** for infectious agent and pathogen abbreviations and **Supplementary Material, Table 3** for all prevalences.

Among the eukaryotic parasites, *Loma* sp. (lo_sal; 19%–67%), *Ichthyophonus hoferi* (ic_hof; 29%–59%), and *Parvicapsula pseudobranchicola* (pa_pse; 16%–27%) were detected in moderate to high prevalence in all four salmon species (**Fig. 1**). *Ichthyobodo* sp. (ICD; 14%–30%) was detected at moderate prevalence in pink, chum, and coho but was rarely detected in sockeye (3%; **Fig. 1**). *Sphaerothecum destruens* (sp_des) was particularly prevalent in sockeye (25%) but rarely encountered in coho, pink, and chum (5%–1%; **Fig. 1**; **Supplementary Material, Table 3**). The remaining saltwater transmitted parasites showed more specific species distributions, with *Myxobolus insidiosus* (my_ins; 1%–4%) and *Parvicapsula kabatai* (pa_kab; 3% and 2%) detected only in chum and coho, *Kudoa thyrsites* (ku_thy; 4% and 1%) detected in pink and coho, and *Paranucleospora theridion* (pa_ther) detected only in coho salmon (6%; **Fig. 1**; **Supplementary Material, Table 3**). Freshwater transmitted parasites, *Parvicapsula minibicornis* (pa_min) and *Ichthyophthirius multifiliis* (ic_mul), were detected only rarely in coho and sockeye (1%–9%), whereas *Ceratanova shasta* (ce_sha) was detected only in chum and coho (10% and 4% prevalence respectively) and *Nanophyetus salmincola* (na_sal; 1%) only in coho (**Fig. 1**; **Supplementary Material, Table 3**). Notably, all coho with *M. insidiosus, I. multifiliis,* and the majority with *P. minibicornis* detections originated from southern stocks from the Columbia

and Yaquina rivers, whereas all *P. kabatai* and *S. destruens* detections were in fish from Northern British Columbia and Alaskan stocks.

Six viruses were detected in salmon from the GoA, although most only in a single species (**Fig. 1**; **Supplementary Material, Table 3**). The exception was encephalopathy and retinopathy virus (VER), highly prevalent in coho (36%) but also detected in sockeye and chum (2% and 1%; **Fig. 1**). Sockeye salmon was the only species where Pacific salmon parvovirus (PSPV) (39%) and a Putative-Picorna virus (Picorna2) (2%) were found (**Fig. 1**). Three viruses were exclusively observed in coho salmon: SalmovirusWFRC1_virus (5%), erythrocytic necrosis virus (ENV) (3%), and an uncharacterized Rhabdovirus (1%; **Fig. 1**). No viruses were detected in pink salmon (**Fig. 1**).

Infectious agent profiles of salmon in the GoA differ from Coastal waters

To determine how salmon infectious agents may shift between the coastal margin and the deeper off-shore waters, we compared the prevalence of infectious agents in salmon in the GoA and Coastal British Columbia (**Fig. 1**).

Ichthyophonus hoferi was significantly more prevalent in the GoA in all four species, with pathogen loads in pink, coho, and chum higher than any observed on coastal waters (**Figs. 1** and **2a**). Sockeye and coho with high *I. hoferi* loads showed systemic infection as seen by multiple granulomatous inflammatory foci in several organs (**Supplementary Material, Figs. 4a and 4b**).

Similarly, *Loma* sp. was present at loads higher than typically seen in coastal waters for coho, chum, sockeye, and pink, with prevalence being significantly higher in the GoA for the latter three species (**Figs. 1** and **2a**). High loads corresponded with abundant gill xenomas in coho and sockeye that were absent from individuals without *Loma* sp. detections (**Supplementary Material, Figs. 4c and 4d**).

Other pathogens with significantly higher GoA prevalence in individual species were *S. destruens* in sockeye, *Ca.* B. *cysticola* in pink, *C. shasta* in chum, and VER in coho (**Fig. 1**). The latter virus was also observed at unusually high loads in the GoA (**Fig. 2a**). *P. pseudobranchicola*, detected in GoA chum, has not been detected in chum in coastal waters, but has been found in other Pacific salmon species.
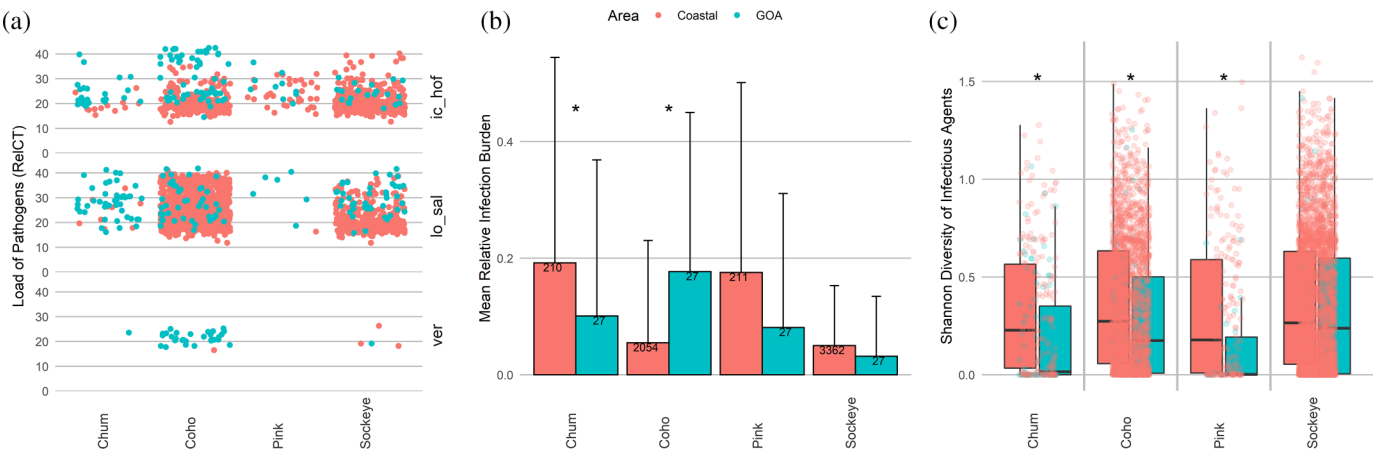
Fig. 2. (a) Selected pathogens showing extremely high loads in samples from the Gulf of Alaska (GoA): ic_hof, *Ichthyophonus hoferi*; lo_sal, *Loma* sp.; ver, Viral encephalopathy and retinopathy virus. (b) Relative infection burden of salmon in the GoA compared with coastal British Columba (BC; mean value, SD, and *n*). (c) Shannon diversity of infectious agents and pathogens of salmon in the GoA compared to coastal BC (mean value, SD). Asterix indicates significant differences with a *t*-test $p < 0.05$.

There were numerous infectious agents and pathogens more prevalent in coastal salmon than GoA. Among marine transmitted parasites, *P. theridion* was significantly lower in prevalence in all species in the GoA and *P. kabatai* was lower in sockeye, pink, and chum (**Fig. 1**). Among freshwater transmitted parasites, *P. minibicornis* was observed at reduced prevalence in GoA sockeye and chum and was absent in GoA coho, whereas *Myxobolus arcticus* was absent from all species, likely due to brains not being sampled in this screen. *Ca.* B. *cysticola* showed lower prevalence in GoA coho and sockeye (**Fig. 1**). Salmon pescarenavirus-2 showed lower prevalence in GoA chum and sockeye than in coastal regions (**Fig. 1**). Other pathogens with reduced prevalence in the GoA were ENV and *C. shasta* in sockeye, *P. pseudobranchicola*, *Tenacibaculum maritimum*, and *Tetracapsuloides bryosalmonae* in coho and *Ca.* S. salmonis in chum (**Fig. 1**).

Three recently discovered viruses that have not yet been surveyed in salmon on the coastal margin were detected in salmon in the GoA, including a Putative-Rhabdovirus and Salmovirus WFRC1 in coho and Putative-picorna virus in sockeye (**Fig. 1**).

Together, chum, pink, and sockeye showed lower RIB in the GoA compared with coastal British Columbia, Canada, with the difference being significant for chum salmon (**Fig. 2b**). In contrast, RIB in coho was significantly higher in the GoA than in coastal waters (**Fig. 2b**), although the number of infectious agents as well as their diversity within individual fish was significantly lower in the GoA for all species except sockeye (**Figs. 2c** and **2d**). This suggests that the higher RIB in coho in the GoA is due to the higher loads of VER, *Loma* sp., and *I. hoferi*. Only sockeye showed no significant differences in infectious agent number or diversity between the coast and the GoA (**Figs. 2c** and **2d**).

Differential gene expression provides clues on stressors experienced by salmon in the GoA

Prey availability, temperature-related factors, and infectious agent profile correlate with differential gene expression of salmon in the GoA

To investigate stressors of salmon in the GoA, we compared the expression of all genes from all biomarker panels across all individuals of the same species. First, we visualized gene expression using heatmaps, also displaying pathogen detections as well as co-varying metadata (**Fig. 3**). Hierarchical clustering of gene expression allowed us to identify clusters of salmon showing similar expression patterns (**Fig. 3**). In chum, clusters four and five showed markedly reduced overall gene expression that was associated with elevated RIB and lower biomass of hydromedusa at capture location, the primary prey of chum salmon (Somov et al. 2019), as well as lower levels of dissolved oxygen (**Fig. 3**; **Supplementary Material, Fig. 5**). Further, temperature at site of capture was also significantly associated with overall gene expression, with warmer temperatures correlating to higher gene expression (**Fig. 3**; **Supplementary Material, Fig. 5**). Similarly, in sockeye, elevated temperature, and prey availability (e.g., small zooplankton) was associated with a global increase in gene expression (**Fig. 3**; **Supplementary Material, Fig. 6**). Condition factor K was significantly covaried between clusters in sockeye (**Fig. 3**; **Supplementary Material, Fig. 6**). Coho salmon showed no large-scale changes in gene expression and clusters differed primarily in the response of individual biomarkers to RIB and prey availability (**Fig. 3**; **Supplementary Material, Fig. 7**). Pink salmon also showed large-scale changes to gene expression associated with RIB, prey availability, and temperature, but interestingly high values of these factors were associated with reduced global gene expression rather than an increase as had been seen in chum and sockeye salmon (**Fig. 3**; **Supplementary Material, Fig. 8**).

Next, we performed a PCA to ordinate gene expression profiles of individual salmon. We focused on the first four principal components to identify dominant biomarker panels driving differential gene
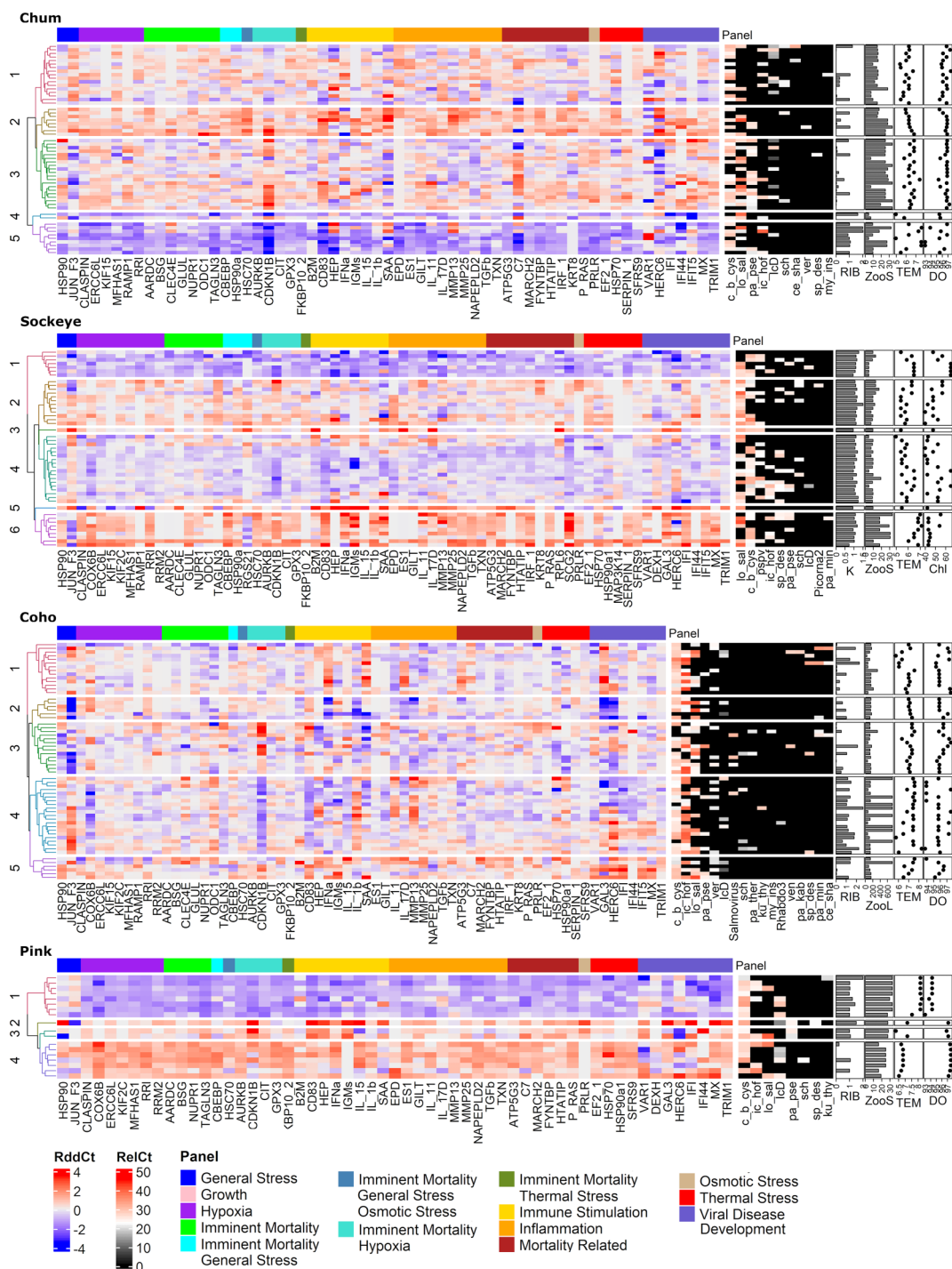
Fig. 3. Gene expression and pathogen profile heatmap of overwintering salmon in the Gulf of Alaska (GoA). Gene expression of salmon is depicted in the left heatmap, where the relative delta–delta cycle threshold value (RddCt) detected in the Fit-Chip analysis is shown (blue to red) and individuals (rows) are hierarchically clustered based on similarities in gene expression (dendrogram and cluster number on left). Columns correspond to genes and are sorted by Fit-Chip biomarker panel (color scheme above). Load of pathogen detections associated with the individuals are depicted on the right heatmap in relative cycle threshold value (RelCt, black to red). Annotation graphs to the far right show relative infection burden (RIB), temperature (TEM) at the capture site, dissolved oxygen saturation (DO), and zooplankton size class abundance (ZooS/L).

expression. We then tested observational data on salmon health and condition as well as oceanographic data for correlations with principal components and plotted significantly correlated data scaled and directional on the ordination plots to depict the direction of correlation. In the last step, we queried what genes showed changes in expression correlated with the superimposed data by using a Euclidean distance-based approach or plotted a vector summarizing of all genes of a biomarker panel, respectively (**Fig. 4**; **Supplementary Material, Fig. 9**). By visualizing the hierarchical clusters identified earlier, this allowed us to identify the environmental factors and pathogens associated with the differential gene expression providing a population scale overview of stressors of overwintering salmon (**Fig. 4**; **Supplementary Material, Fig. 9**).

Differential gene expression in chum salmon was primarily driven by variations in biomarkers for inflammation (MMP13, NAPEPLD2, TXN, GILT), immune stimulation (SAA, CD83, IFNa), mortality-related (C7, P_RAS), viral disease development (VDD) biomarker panels (HERC6, IFIT5, IFI44, VAR1), followed by imminent mortality and hypoxia (TAGLN3, CDKN1B; **Fig. 4a**; **Supplementary Material, Fig. 9a**). Along PC1, these factors explained 36% of the variation in gene expression. Chum clusters four and five showed lower gene expression across all biomarker panels and clustered on the positive end of PC1 (**Figs. 3** and **4a**; **Supplementary Material, Fig. 9a**). Inflammation (MMP13, NAPEPLD2, TXN) and immune stimulation biomarkers (SAA) contributed the negatively to PC2 (10.8% explanatory power), while hypoxia and imminent mortality biomarkers (CDKN1B) contributed positively (**Figs. 3** and **4a**; **Supplementary Material, Fig. 9a**). RIB as well as nematode prevalence was correlated with lower overall gene expression in individuals of cluster four and five, but positively associated with inflammation (MMP13, NAPEPLD2), immune stimulation (SAA), and VDD (HERC6, IFIT5) markers on PC2. Conversely, pathogens *P. pseudobranchicola* (pa_pse) and *S. destruens* (sp_des) were negatively associated with these immune response markers along PC2 (**Fig. 4a**; **Supplementary Material, Fig. 9a**). Biomass of hydromedusae (Medu) and other the prey of chum (small zooplankton: Zoo_S) was positively correlated with global upregulated gene expression along PC1 and lower expression of the immune response markers associated with PC2 (Somov et al. 2019), while being directly opposed to RIB and nematode prevalence across PC1 and PC2 (**Fig. 4a**; **Supplementary Material, Fig. 9a**). Principal components three and four (explaining 10% and 6.2%, respectively) were driven by the same genes driving PC1 and PC2; however, inflammation and VDD markers were opposing each other along PC3, with inflammation driven by individuals of cluster four, that showed enlarged gallbladders (a sign of prolonged low stomach fullness) and larger size (Mass) and smaller individuals at higher temperature associated with VDD expression (**Fig. 4b**; **Supplementary Material, Fig. 9b**). PC4 was driven by opposing trends of immune stimulation and hypoxia biomarkers, primarily associated with zooplankton (euphausiids and medium size zooplankton; **Figs. 3** and **4b**; **Supplementary Material, Fig. 9a**).

Sockeye showed similar patterns to chum salmon with two clusters (one and four) showing reduced overall gene expression associated with the positive end of PC1 (43.8%). The primary drivers associated with these global expression changes were the biomarker panels immune stimulation (B2M, HEP, IGMs, CD83, SAA), inflammation (IL_17D, ES1), mortality related (SCG2, RPL6), VDD (HERC6, DEXH, MX, IFI), and a group of hypoxia genes (RRl, CLASPIN, KIF15, COX6B, RRM2) (**Fig. 4c**; **Supplementary Material, Fig. 9c**). These hypoxia genes were also major contributors to PC2 (13.8%) opposed by the general stress marker JUN_F3 (**Fig. 4c**; **Supplementary Material, Fig. 9c**). Globally lowered gene expression in sockeye clusters one and four was associated with lower abundance of small zooplankton (Zoo_S), pteropods (Ptero), and hydromedusae (Medu) along PC1, and to a lesser degree lower temperature at site of capture (**Fig. 4c**; **Supplementary Material, Fig. 9c**). Euphausiids (Euphaus) that were identified as the primary prey of sockeye, were correlated with the positive end of PC2, opposed to temperature, and showed increased expression of inflammation and immune stimulation markers, but showed weaker association with gene expression than other
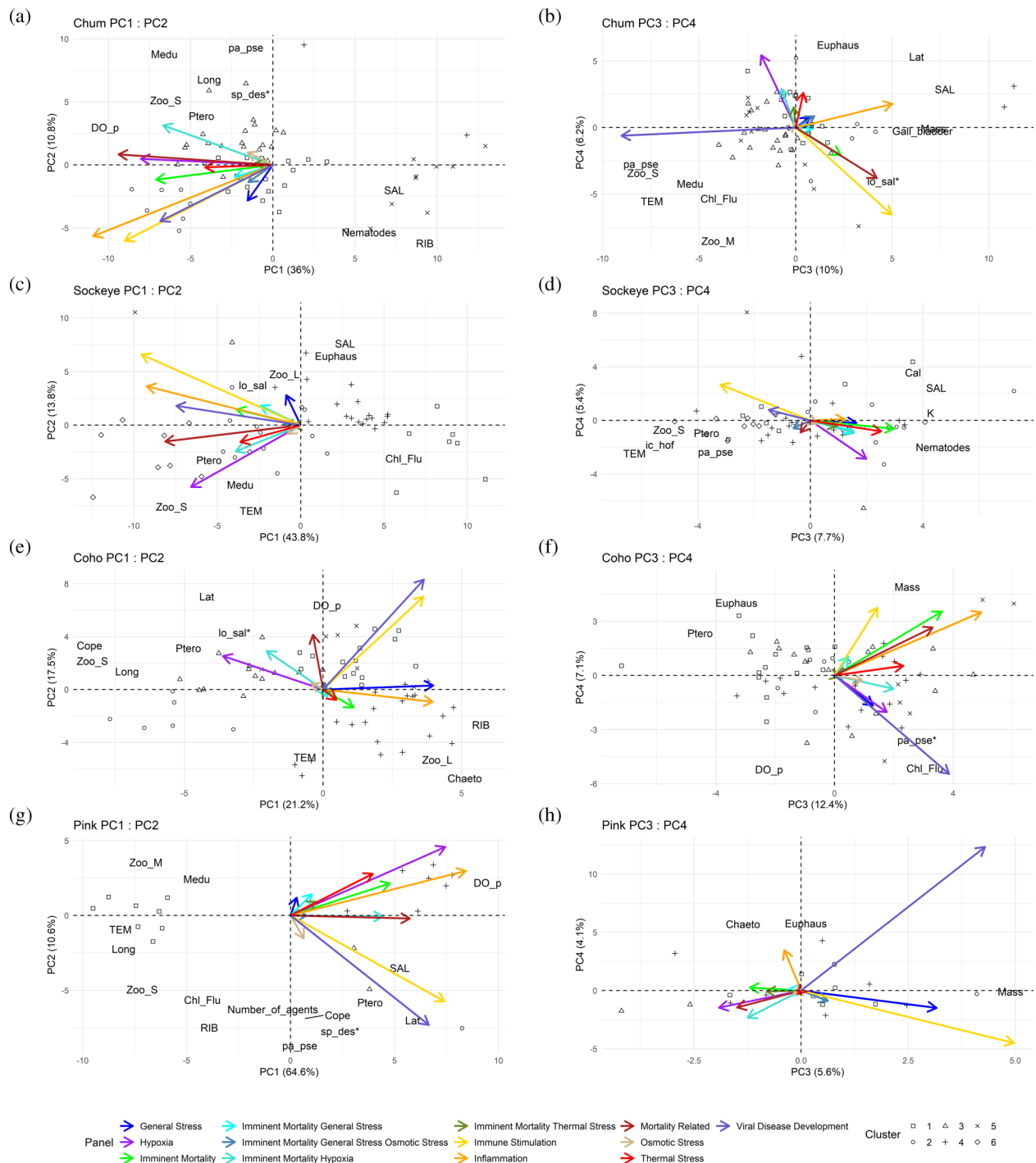
Fig. 4. Gene expression analysis of salmon captured in the Gulf of Alaska during the winter 2019. (a) and (b), chum; (c) and (d), sockeye; (e) and (f), coho; (g) and (h), pink. PCA plot of gene expression is overlaid with meta-data (infectious agents, intrinsic variables, and environmental metadata). Dots depict individual salmon. Annotations (bold black) show superimposed data correlating with differential gene expression. Only data with a correlation significance of $p < 0.05$ are shown unless noted with "*". Gene expression influence summarized by biomarker panels are indicated by the colored vectors (see main text for description of specific biomarkers driving these findings). For a full figure depicting individual genes see **Supplementary Material, Fig. 9**. For a full list of infectious agent abbreviations and corresponding factors see **Table 1**.

prey groups (Fig. 4c; Supplementary Material, Fig. 9c). The prevalence of the gill parasite *Loma spp.* (lo_sal) was associated with expression of inflammation and immune stimulation biomarkers along PC1 and PC2. Principal component three (7.7% exploratory power) saw a strong correlation of immune stimulation (SAA, IFNa, IGM) and inflammation biomarkers (IL_17D, MMP24, MMP13) with the parasites *I. hoferi* and *P. pseudobranchicola*, whereas inflammation (ES1, EPD) and imminent mortality markers (TAGLN3, RGS21) were associated with nematode prevalence (Fig. 4d; Supplementary Material, Fig. 9d). Fish with higher caloric content and better condition factor (K) were also associated with lower temperatures at site of capture and lower prevalence of pathogens (ic_hof, pa_pse) (Fig. 4d; Supplementary Material, Fig. 9d).

Differential gene expression in coho salmon showed a nuanced response of biomarker panels along the first two principal components where inflammation (MMP13, IL_11, NAPEPLD2, IL_17D), general stress (JUN_F3), immune stimulation (IL_1b, HEP, SAA, IFNa), and VDD (HERC6, GAL3) associated positively with RIB and fish of cluster four on the positive end of PC1 (21.2%; Fig. 4e; Supplementary Material, Fig. 9e). RIB was inversely related to the biomass of pteropods (ptero) that were the preferred prey of coho salmon in GoA in 2019 (Somov et al. 2019), with fish from cluster four experiencing the lowest pteropod biomass (Fig. 4e; Supplementary Material, Fig. 9e). Hypoxia biomarkers (COX6B, RRM2, CDKN1B) were correlated with the prevalence of the gill parasite *Loma* sp. (lo_sal) along PC1 and PC2 (17.5%) (Fig. 4e; Supplementary Material, Fig. 9e), specifically amongst individuals of clusters two, three, and five. Principal components three and four (12.4% and 7.1%, respectively) showed a global increase in expression that was associated with the size of fish (Mass) of individuals in cluster four, as well as an increased expression of VDD biomarkers related to *P. pseudobranchicola* (pa_pse) load (Fig. 4f; Supplementary Material, Fig. 9f).

Pink salmon of cluster one showed reduced global gene expression compared to other clusters, grouped along the negative spectrum of PC1 (64.6 %) and were associated with higher temperatures, higher RIB, and higher biomass of prey species (Fig. 4g; Supplementary Material, Fig. 9g). On the positive spectrum of PC1, clusters two, three, and four were associated with increased expression imminent mortality markers (CDKN1B, CBEBP, GPX) but were differentiated along PC2 (10.2%) with expression of hypoxia (COX_6B, RRI, GPX), and inflammation biomarkers (NAPEPLD2, IL_17D) were associated with cluster four, while clusters two and three showed increase expression of VDD (TRIM, GAL3, MX, VAR1, IFI) and immune stimulation markers (SAA, IGMs, HEP, CD83) that were associated with increased RIB, number of infectious agents, as well as the prevalence of the parasites *S. destruens* (sp_des) and *P. psudobranchiola* (pa_pse) (Fig. 4g; Supplementary Material, Fig. 9g). Principal component three (explaining 5.6%) showed elevated expression of VDD (GAL3, Mx, IFI, HERC6), immune stimulation (SAA, IL_15), and general stress genes (HSP90) along the positive end of PC3, which was correlated with larger individuals (Mass; Fig. 4h; Supplementary Material, Fig. 9h). Higher biomass of Euphausiids (Euphaus) along PC4 (4.1%) correlated with VDD expression and inflammation (EPD).

To highlight overlying trends of pathogens and environmental factors such as prey biomass and temperature, we plotted the biomass of primary prey species in relation to ocean temperature and RIB across the first two principal components of gene expression (Fig. 5; Supplementary Material, Fig.10). Since global depression of immune response genes (immune stimulation, inflammation, and viral disease development) effectively equals immunosuppression, we created the inverse vector of gene expression of said biomarker panels to depict this suppressed immune status. Indeed, immunosuppression showed an inverse relationship with the biomass of the primary prey species as well as a direct correlation with RIB in all species (Fig. 5). In chum and pink salmon this trend dominated gene expression along PC1 (Fig. 5). Coho showed a strong inverse correlation between primary prey biomass and RIB, but immunosuppression was only weakly associated with them along PC2,

suggesting that large-scale changes in gene expression resulting in immunosuppression are subordinate to other factors relating to RIB (Fig. 5). In sockeye, gene expression patterns were more strongly associated with small zooplankton, rather than the primary stomach content which was Euphausiids (Fig. 5). Accordingly, lower biomass of small zooplankton was associated with immunosuppression and elevated RIB in sockeye along PC1 (Fig. 5). Coho and pink salmon that were primarily caught along the southern border of the distribution area and experienced the highest ocean temperatures and showed a strong correlation of immunosuppression and RIB with increased temperature (Fig. 5).

Infectious agent profiles correlated with gene response to viral and gill infections and stock of origin in coho

To determine if infectious agent profiles were associated with environmental factors and gene expression, we visualized the gene expression data in rank order-based NMDS-ordinated pathogen profiles of individuals by species (Fig. 6).

Differences in chum infectious agent profiles were primarily driven by *C. shasta* (ce_sha) with minor opposing contributions of *P. pseudobranchicola* (pa_pse) and *S. destruens* (sp_des) along NMDS1 (Fig. 6a). *C. shasta* was only found in individuals of gene expression cluster one and was associated with the expression of a mortality-related biomarker (MARCH2) (Fig. 6a). NMDS2 differentiation was driven by *Loma* sp. (lo_sal) and *P. pseudobranchicola* (pa_pse) on the positive end of NMDS2 that were correlated with larger individuals (Mass; Fig. 6a). Smaller individuals on the negative end of NMDS2 were associated with *Ca. S. salmonis* (sch) and *Ca. B. cysticola* (c_b_cys), as well as the expression of imminent mortality/hypoxia (GPX3) and inflammation (EPD) biomarkers.
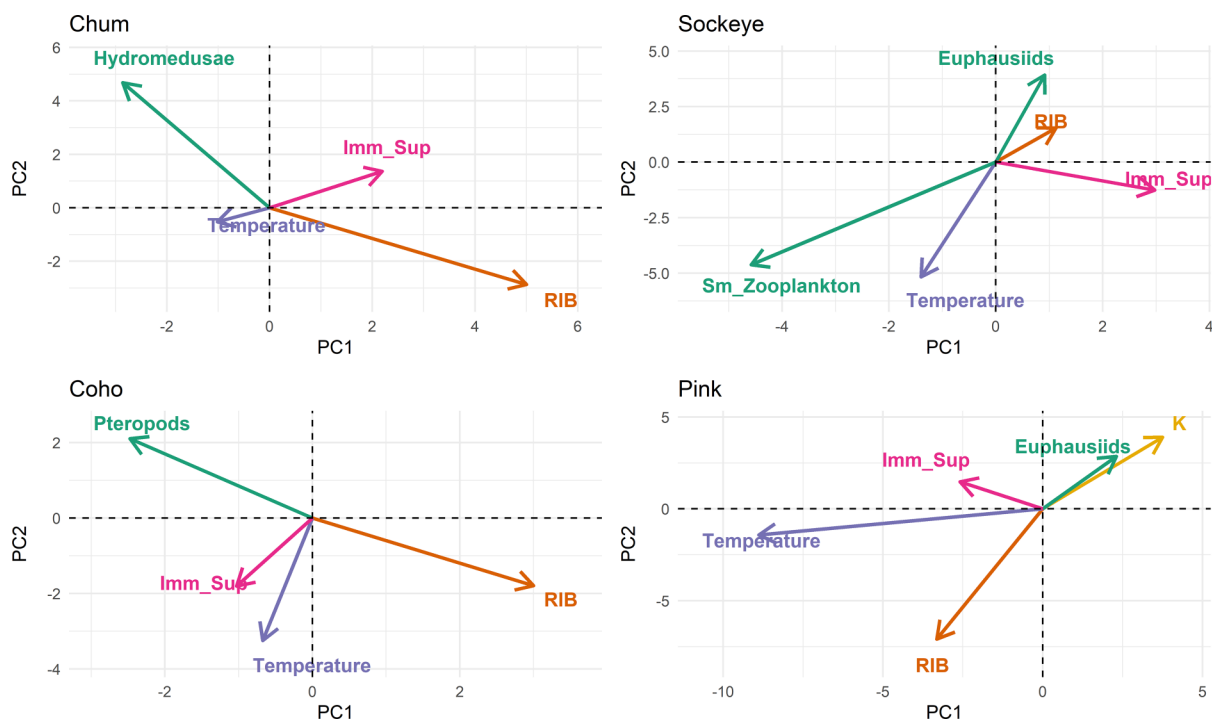
Fig. 5. Association of primary prey species biomass, relative infection burden, and temperature with gene expression in the Gulf of Alaska during the winter 2019. Primary prey species such as euphausiids, hydromedusae, and pteropods are highlighted in relation to immunosuppression (Imm_Sup: inverse vector of summarized biomarker panels immune stimulation, inflammation, and viral disease development).
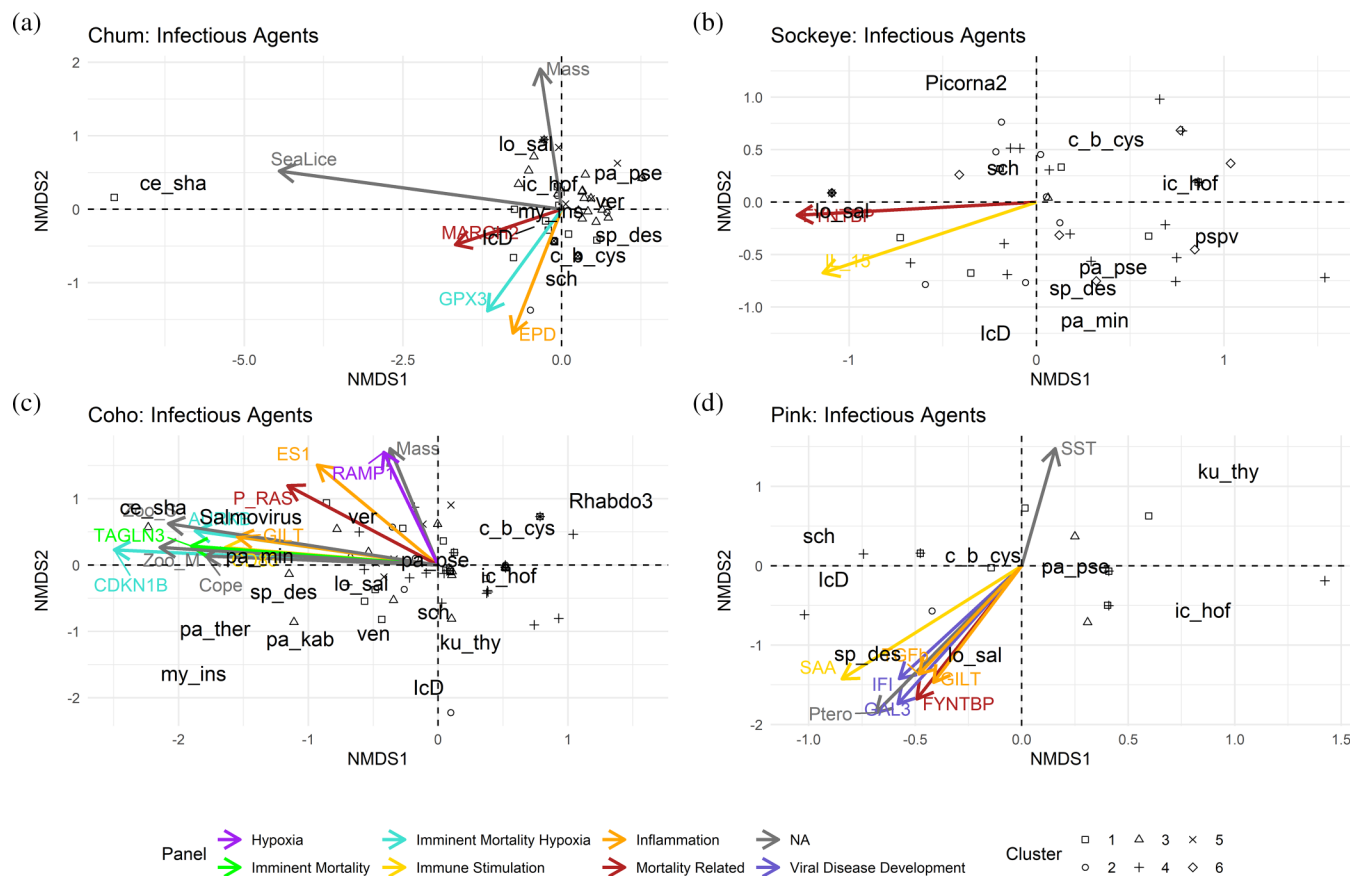
Fig. 6. Nonmetric multidimensional scaling of infectious agent profile overlaid with corresponding gene expression, intrinsic and environmental metadata. Dots depict individuals and infectious agent vectors are indicated by the infectious agent abbreviation (see Table 1 for abbreviations). Corresponding superimposed data with a significance of $p < 0.05$ is depicted.

Sockeye infectious agent profiles differed primarily by the opposing trends of *Loma* sp. (lo_sal) against PSPV and *I. hoferi* (ic_hof) along NMDS1 with mortality related (FYNTBP) and immune stimulation biomarkers (IL_15) associated with *Loma* sp. (Fig. 6b). Differences across NMDS2 were driven by Putative-picornavirus (Picorna2), *Ichthyobodo* sp. (IcD), and *P. minibicornis* (pa_min) (Fig. 6b).

Stock of origin was significantly associated with pathogen profile variation in coho salmon. Accordingly, the pathogen profiles were primarily differentiated by rare and stock-specific pathogens such as *C. shasta* (ce_sha), Salmovirus, *P. minibicornis* (pa_min), *P. theridion* (pa_ther), and *M. insidiosus* (my_ins) along the negative end of NMDS1, present in only a few individuals each; the latter three pathogens were only found in fish originating from within the contiguous United States (Fig. 6c). Correlating gene expression was seen in genes from biomarker panels imminent mortality and hypoxia (CDKN1B, TAGLN3, AURKB), inflammation (GILT, ES1), immune stimulation (CD83), mortality-related signature (P_RAS), as well as the prevalence of medium-sized and small zooplankton (Zoo_S/M) (Fig. 6c). Hypoxia gene expression (RAMP1) was correlated with large individuals along NMDS2, while small individuals were associated with *Ichthyobodo* sp. (IcD) (Fig. 6c).

Infectious agent profiles in pink salmon differed primarily in the presence of Ca. S. *salmonis* (sch), *S. destruens* (sp_des), and *Ichthyobodo* sp. (IcD) opposed by *I. hoferi* (ic_hof) and *K. thyrsites* (ku_thy) along NMDS1 (**Fig. 6d**). Immune stimulation (SAA), inflammation (TGFb, GILT), VDD (IFI, GAL3) and mortality related biomarkers (FYNTBP) were correlated with the gill pathogen *Loma* sp. (lo_sal) and *S. destruens* (sp_des) and at higher abundance of pteropods (Ptero) and lower sea surface temperature (SST; **Fig. 6d**).

Discussion

The GoA is the main overwintering habitat for North American origin Pacific salmon stocks as well as a significant proportion of Asian origin chum salmon. To better understand factors that may contribute to changes in ocean survival, it is critical to monitor the health and condition of salmon in this environment, specifically during the winter months that are thought to be a critical time period for first-year fish (Beamish and Mahnken 2001). Here we report the first comprehensive overview on the health and condition of Pacific salmon during the 2018–2019 winter period in the GoA, illustrating the linkages between food limitations, immunosuppression, and infective burdens in ocean-dwelling salmon.

Most high prevalence pathogens could be acquired by trophic transmission in the GoA

RIB of microparasites in the GoA was lower compared with coastal samples in all species except coho, which had a significantly higher relative infection burden due to high prevalence of the virus VER as well as the parasites *I. hoferi* and *Loma* sp. These two parasites and the bacterium *Ca.* B. *cysticola* were the highest prevalence pathogens in the GoA across all species.

Ichthyophonus hoferi was present at significantly higher prevalence and load in all salmon in the GoA compared with coastal areas. This common parasite causes systemic disease in marine fish and is thought to transmit trophically (Hershberger et al. 2002; Bass et al. 2017). This suggests that the GoA is a reservoir for this parasite and that piscivorous species acquire infection through their prey. *Ichthyophonus hoferi* detections in chum salmon, a species with low proportion of fish in its diet (1.8% in the study area) is surprising but suggests very high *I. hoferi* prevalence in prey species (Somov et al. 2019). Sockeye showed significant stimulation of immune and inflammatory genes associated with *I. hoferi* prevalence.

Similar to *I. hoferi,* the microsporidian parasite *Loma* sp. (most likely *Loma salmonae*) was present at significantly higher prevalence and load in all salmon in the GoA compared with coastal areas (Shaw et al. 2000). This parasite can result in respiratory distress, impaired swimming, and reduced growth rates (Shaw et al. 2000). Transmission is initiated by release of spores from ruptured gill xenomas and is completed by the spores infecting the pillar and endothelial cells of the gills of a new host (Shaw et al. 1998). In the GoA, coho showed significant correlation of gene expression profiles with *I. hoferi* prevalence.

The bacterium *Ca.* B. *cysticola* causes epitheliocystis in gill tissue of salmonids and is associated with proliferative gill inflammation (Toenshoff et al. 2012; Mitchell et al. 2013). This bacterium is commonly encountered in Pacific salmon and was only significantly elevated in prevalence in pink salmon in the GoA (Bass et al. 2017; Teffer et al. 2017). *Ca.* B. cysticola has been correlated with lower relative weight (Bass et al. submitted), inflammation in coastal Chinook (Wang et al. 2018), and reduced migration success in steelhead (*Oncorhynchus mykiss*) (Twardek et al. 2019).

Viral encephalopathy and VER was significantly elevated in prevalence in coho salmon. This widespread virus of marine fish and invertebrates is transmitted horizontally, vertically, and trophically

(Costa and Thompson 2016). While brain tissue was not included in this screen, in contrast to coastal salmon, the neurotropic VER can also be detected in other tissues by qPCR (Costa and Thompson 2016). We hypothesize that the detection of VER in non-neuronal tissue could reflect a systemic viremia state of recent trophic acquisition, but we likely underestimate both the prevalence and load of this virus in GoA. The relatively high prevalence in coho salmon might reflect their higher trophic level compared with other salmon species encountered in the GoA (Somov et al. 2019).

ENV often causes epizootics in Pacific herring but has recently established as a common coastal virus infecting salmon (Pagowski et al. 2019). It was found in lower prevalence in the GoA, potentially due to the more coastal distribution of Pacific herring not commonly found in the open ocean limiting transmission potential.

The meso/mycetozoea protist *Sphaerothecum destruens,* transmitted in fresh water in a broad host range of fish, was found at significantly elevated prevalence in sockeye salmon (Gozlan et al. 2009). Infection results in splenomegaly and nephromegaly and causes anemia (Elston et al. 1986). The elevated prevalence in sockeye in the GoA might be a stock of origin, as the GoA has a high proportion of Alaskan origin fish that harbor this infection, compared with the prevalence of British Columbia origin fish in the coastal database.

Ichthyobodo sp. was detected at high prevalence in pink, chum, and coho salmon. This ectoparasite has been shown to be a major factor influencing chum survival at sea in the western Pacific (Urawa 1993; Mizuno et al. 2017).

Interpreting the prevalence data in the GoA compared with coastal British Columbia needs to consider the differences in life stage and season. GoA fish were captured in the middle of their life, whereas coastal salmon from British Columbia were primarily out-migrating post-smolts. As salmon change their diet throughout their life, e.g., increase piscivory, this might impact exposure to trophically transmitted pathogens. The heterogeneity between data sets is especially pronounced for sockeye, pink, and chum salmon that spend most of their life in the open ocean and are only rarely encountered in coastal waters. Coho salmon, on the other hand, are present in coastal waters at all life stages and offer a more robust comparison. Thus, seasonal patterns and fish size or age might influence differences in infectious agent prevalence, specifically for sockeye, pink, and chum.

Infectious agents of freshwater and coastal origin decline in prevalence in the GoA

Myxozoans, commonly observed in coastal environments, have a life cycle that alternates between fish and invertebrate hosts. Most myxozoans, specifically all *Parvicapsula spp.,* showed reduced prevalence in the GoA as invertebrate hosts such as annelids may be limiting (Yokoyama, Grabner and Shirakashi 2012; Somov et al. 2019). As *Parvicapsula spp.* can reduce visual acuity and have been correlated with increased predation, infected individuals might also be lost from the population (Miller et al. 2014; Nylund et al. 2018). *P. kabatai* and *P. minibicornis* both showed stock-specific trends in coho. *Tetracapsuloides bryosalmonae*, the causative agent of the lethal proliferative kidney disease was absent in the GoA, with infected individuals presumably removed from the population (Sterud et al. 2007).

PSPV, a DNA virus reported in sockeye salmon with unknown pathogenicity, was the highest prevalence virus in the GoA (Miller et al. 2011, 2017; Nekouei et al. 2018). Several novel viruses, Salmovirus and Rhabdo virus, were detected in GoA coho correlating with hypoxia stress and VDD gene expression, as well as a novel Picornavirus in chum (Mordecai et al. 2019, 2020).

The microsporidian *P. theridion (*syn. *Desmozoon lepeophtherii),* infects gill tissue but also the sea louse *Lepeophtheirus salmonis* that may act as a vector (Nylund et al. 2010; Sveen et al. 2012). *P. theridion* is highly prevalent in coastal salmon in spring and summer but decreases over winter and was only observed in five coho in the GoA (Tucker et al. 2018; Laurin et al. 2019; Bateman et al. 2020).

The bacterium *Ca.* S. salmonis (Sch), which causes gill impairment, was lower in prevalence in in the GoA (Nylund et al. 2015), as was *T. maritimum*, the causative agent of mouth rot, presumptively related to the poor outcome of these diseases (Avendaño-Herrera et al. 2006).

Infectious agent profiles are associated with size and in some species stock of origin

In chum and coho salmon, infectious agent and gene expression profiles significantly correlated with size, suggesting that many infectious agents are either shed during maturation or that infected individuals are lost from the population due to mortality. Alternatively, differing prey composition (Losee et al. 2014) or age-dependent mixture such as in chum where Asian origin fish are absent from the first-year age class might explain these trends. Coho salmon showed stock-specific differences in infectious agent profile, with stocks from the contiguous United States showing distinct infectious agent profiles compared to stocks from Northern British Columbia and Alaska.

Prey availability and temperature are correlated with immunosuppression and higher pathogen prevalence in Pacific salmon in the GoA

Changes of the physical environment experienced by salmon at sea based on daily travel rates are negligible (0%–1% on average: **Supplementary Material, Table 4**, **Supplementary Material, Fig. 11**) in relation to the speed of gene expression changes that can occur in response to stress in salmonids (Ogura and Ishida 1992; Ogura and Ishida 1995; Houde, Akbarzadeh, et al. 2019). While the abundance of prey items was more spatially variable (3%–28% changes per day on average: **Supplementary Material, Table 4**, **Supplementary Material, Fig. 11**), the movement of salmon at sea is not random and salmon are expected to remain in prey rich areas, once found, thus the correlation of gene expression with prey group presence might be stronger than apparent from prey distribution.

Fit-Chip analysis in all species showed large-scale changes in gene expression, specifically from biomarker panels involved in immune response (immune stimulation, inflammation, VDD). In pink, and to a lesser degree in coho salmon primarily caught in warmer waters on the southern border of the survey area, reduced gene expression correlated with warmer temperatures and reduced prey availability. This could be an indicator of higher metabolic demands in malnourished individuals. In chum and sockeye, gene expression correlated positively with temperature, whereas low prey availability still showed a negative correlation. At lower temperatures, gene expression may simply reflect the correlation of metabolic activity with temperature in ectothermic animals. Alternatively, individuals at higher latitudes (i.e., colder waters) were experiencing extremely high abundance of the northern sea nettle *Chrysaora melanaster*, a large jellyfish (Pakhomov et al. 2019). Thus, temperature might act as a proxy for the impact these large jellyfish had on zooplankton communities thereby affecting lower trophic level salmon in the north of the GoA. Indeed, chum followed by sockeye had the lowest stomach fullness indices (Somov et al. 2019). Individuals with reduced expression of most immune response genes are effectively immunosuppressed. Immunosuppression was correlated inversely with the biomass of the primary prey groups as determined by stomach content in all species except sockeye where small zooplankton had a larger effect than euphausiids, the dominant stomach

content of sockeye (Somov et al. 2019). Immunosuppression was strongly correlated with RIB in chum and pink salmon, and to a lesser degree in coho and sockeye. Pink salmon also showed a protective effect of high condition factor that countered immunosuppression and RIB.

Multiple ecological relationships could explain the observed link between energetics (prey availability), immunosuppression, RIB, and temperature. Low prey availability could drive salmon into energetic deficit, to which they respond by suppressing the immune system, a common response to malnutrition in many vertebrates (Latshaw 1991; Lord et al. 1998). Similar observations have been made in steelhead/rainbow trout, where fish exhibit distinct immunity and energetic programs in response to smoltification and migration (Sutherland et al. 2014), as well as in Atlantic salmon where starvation negatively impacted immune response to bacterial infection (Martin et al. 2010). Strikingly, immunosuppression has recently been associated with mortality in Atlantic salmon (Krasnov et al. 2020). Immunosuppression would make salmon more susceptible to pathogens, explaining the elevated infectious agent loads. Immunosuppression could also explain the absence of immune response to pathogens such as *Ca.* B. *cysticola* and *S. destruens*, suggesting that these are opportunistic pathogens with elevated prevalence in immunosuppressed individuals. Since condition factor was inversely correlated with immunosuppression and RIB, "good performance" could have acted protectively, as such individuals are less likely to suffer from energy deficit, thus are immunocompetent and able to fend off infections.

This interpretation is corroborated by field observations, where prey groups showed heterogeneous distributions with little overlap and sockeye and chum salmon exhibited poor feeding condition (Pakhomov et al. 2019; Somov et al. 2019). Specifically in chum, extremely low condition factors individuals were caught where the average water temperature were more than half a degree warmer than their preferred range (Fukuwaka et al. 2007).

Unusually warm temperatures and stratification during the weak 2018–2019 El Niño event—conditions previously hypothesized to disrupt open-ocean food webs and reduce prey availability (Rand 2002; NOAA 2021)—could have driven the observed energy deficits of many salmon in the study area by reducing primary production or altering zooplankton communities. Accordingly, salmon in the survey area were observed to orientate towards structural elements of the water column as well as mixed layer depth, presumably to improve their energetic balance at more favorable environments (Pakhomov et al. 2019; Radchenko et al. 2019). Alternatively, pathogen exposure associated with certain temperature regimes could result in impaired foraging and thereby cause energetic deficits and immunosuppression.

The Fit-Chip technology was developed and validated on the premise of recognizing specific responses based on consistent patterns of coactivation of as few as 7 curated biomarkers (Miller et al. 2017; Houde et al. 2019; Akbarzadeh et al. 2020). However, in the GoA only a subset of any given biomarker panel was co-activated in the first four principal components of gene expression. The observed trends in gene expression were primarily large-scale changes in global gene expression, such as is typical to immunosuppression, rather than responses to specific stressors. One caveat is that this study did not employ known health status controls for different stressors to classify stressor status in individual fish, as these were not available across all four species at the time. We can thus only identify relative differences, rather than classify individuals into specific stressor categories. Refinements of Fit-Chip technology including species-specific stress standards and classification systems are underway.

Cumulative effects of ocean conditions, prey availability, and infectious agents could impact overwintering salmon in the GoA and highlight challenges in a warming ocean

We presented the first comprehensive overview of the health and condition of Pacific salmon at the end of the winter in the open Eastern Pacific Ocean. We highlight overall trends in pathogen profiles and identify key pathogens present in the open ocean. Further, we find that all species are influenced by energetic constraints correlated with reduced prey availability that was associated with immuno-suppression and increased pathogen burden. All species investigated exhibit signs of cumulative effects of stressors, with ocean conditions and prey availability being the primary associated factors. This highlights the impacts a warming ocean could have on winter survival at sea in the face of climate change, specifically in the northern part of the GoA that experienced a large sea surface temperature abnormality in 2019 (Hinch et al. 1995; Miller et al. 2014). Warming, with its downstream effects on salmon energetics, could be especially disruptive in the GoA, where overwintering salmon from both sides of the Pacific basin congregate due to its homogeneous environment (Rand 2002; Beacham et al. 2009; Litzow et al. 2018).

With many wild Pacific salmon populations declining in abundance and productivity, interest in resolving factors that limit salmon survival at sea is strong. Most of what we understand about salmon comes from studies along the coastal margin. The present study provides the first detailed insight into the health and condition of Pacific salmon in the open ocean during the winter. This work will serve as a baseline for future evaluation of the ability of the Northeast Pacific to support salmon populations of North America and Asia.

Acknowledgements

Author contributions

CMD and KMM conceived and designed the study. CMD, ANK, AAS, SE, and EDC performed the experiments/collected the data. CMD, EDC, and KMM analyzed and interpreted the data. KHK, AT, TJM, SL, GM, and AS contributed resources. CMD and KMM drafted or revised the manuscript.

Competing interests

The authors have declared that no competing interests exist.

Data availability statement

All relevant data are within the paper and in the Supplementary Material.

Supplementary material

The following Supplementary Material is available with the article through the journal website at doi:10.1139/facets-2021-0052.

Supplementary Material 1

References

Akbarzadeh A, Günther OP, Houde AL, Li S, Ming TJ, Jeffries KM, et al. 2018. Developing specific molecular biomarkers for thermal stress in salmonids. BMC Genomics, 19: 749. PMID: 30326831 DOI: 10.1186/s12864-018-5108-9

Akbarzadeh A, Houde ALS, Sutherland BJG, Günther OP, and Miller KM. 2020. Identification of Hypoxia-specific biomarkers in Salmonids using RNA-sequencing and validation using high-throughput qPCR. G3, 10(9): 3321–3336. PMID: 32694198 DOI: 10.1534/g3.120.401487

Asahida T, Kobayashi T, Saitoh K, and Nakayama I. 1996. Tissue preservation and total DNA extraction form fish stored at ambient temperature using buffers containing high concentration of urea. Fisheries Science, 62(5): 727–730. DOI: 10.2331/fishsci.62.727

Avendaño-Herrera R, Toranzo AE, and Magariños B. 2006. Tenacibaculosis infection in marine fish caused by Tenacibaculum maritimum: A review. Diseases of Aquatic Organisms, 71(3): 255–266. PMID: 17058606 DOI: 10.3354/dao071255

Bass AL, Bateman AW, Connors BM, Staton BA, Rondeaus EB, Mordecai GJ, et al. Submitted. Identification of infectious agents in early marine Chinook and Coho salmon associated with cohort survival.

Bass AL, Hinch SG, Teffer AK, Patterson DA, and Miller KM. 2017. A survey of microparasites present in adult migrating Chinook salmon (Oncorhynchus tshawytscha) in south-western British Columbia determined by high-throughput quantitative polymerase chain reaction. Journal of Fish Diseases, 40(4): 453–477. PMID: 28188649 DOI: 10.1111/jfd.12607

Bass AL, Hinch SG, Teffer AK, Patterson DA, and Miller KM. 2019. Fisheries capture and infectious agents are associated with travel rate and survival of Chinook salmon during spawning migration. Fisheries Research, 209: 156–166. DOI: 10.1016/j.fishres.2018.09.009

Bateman AW, Peacock SJ, Krkošek M, and Lewis MA. 2020. Migratory hosts can maintain the high-dose/refuge effect in a structured host-parasite system: The case of sea lice and salmon. Evolutionary Applications, n/a(n/a). DOI: 10.1111/eva.12984

Batts WN, LaPatra SE, Katona R, Leis E, Ng TFF, Brieuc MS, et al. 2017. Molecular characterization of a novel orthomyxovirus from rainbow and steelhead trout (Oncorhynchus mykiss). Virus research, 230: 38–49.

Beacham TD, Candy JR, Sato S, Urawa S, Le KD, and Wetklo M. 2009. Stock origins of chum salmon (Oncorhynchus keta) in the Gulf of Alaska during winter as estimated with microsatellites. Bulletin. North Pacific Anadromous Fish Commission, 5: 15–23.

Beacham TD, McIntosh B, and Wallace C. 2010. A comparison of stock and individual identification for sockeye salmon (Oncorhynchus nerka) in British Columbia provided by microsatellites and single nucleotide polymorphisms. Canadian Journal of Fisheries and Aquatic Sciences. Journal canadien des sciences halieutiques et aquatiques, 67(8): 1274–1290. DOI: 10.1139/F10-061

Beacham TD, Wallace C, Jonsen K, McIntosh B, Candy JR, Rondeau EB, et al. 2020. Accurate estimation of Conservation Unit contribution to coho salmon mixed-stock fisheries in British Columbia, Canada using direct DNA sequencing for single nucleotide polymorphisms. Canadian Journal of Fisheries and Aquatic Sciences. Journal canadien des sciences halieutiques et aquatiques, (JA). [online]: Available from nrcresearchpress.com/doi/abs/10.1139/cjfas-2019-0339.

Beamish RJ. 2018. *The ocean ecology of Pacific Salmon and Trout*. American Fisheries Society, Bethesda, MD.

Beamish RJ, and Mahnken C 2001. A critical size and period hypothesis to explain natural regulation of salmon abundance and the linkage to climate and climate change. Progress in Oceanography, 49(1): 423–437. DOI: 10.1016/S0079-6611(01)00034-9

Bettge K, Wahli T, Segner H, and Schmidt-Posthaus H. 2009. Proliferative kidney disease in rainbow trout: time-and temperature-related renal pathology and parasite distribution. Diseases of Aquatic Organisms, 83(1): 67–76.

Cederholm CJ, Kunze MD, Murota T, and Sibatani A. 1999. Pacific salmon carcasses: essential contributions of nutrients and energy for aquatic and terrestrial ecosystems. Fisheries, 24(10): 6–15. DOI: 10.1577/1548-8446(1999)024<0006:PSC>2.0.CO;2

Clarke KR, and Warwick RM. 2001. A further biodiversity index applicable to species lists: Variation in taxonomic distinctness. Marine Ecology Progress Series, 216: 265–278. DOI: 10.3354/meps216265

Cooke SJ, Hinch SG, Donaldson MR, Clark TD, Eliason EJ, Crossin GT, et al. 2012. Conservation physiology in practice: How physiological knowledge has improved our ability to sustainably manage Pacific salmon during up-river migration. Philosophical Transactions of the Royal Society of London. Series B, Biological Sciences, 367(1596): 1757–1769. PMID: 22566681 DOI: 10.1098/rstb.2012.0022

Corbeil S, McColl KA, and Crane MSJ. 2003. Development of a TaqMan quantitative PCR assay for the identification of Piscirickettsia salmonis. Bulletin-European Association of Fish Pathologists, 23(3): 95–101.

Costa JZ, and Thompson KD. 2016. Understanding the interaction between Betanodavirus and its host for the development of prophylactic measures for viral encephalopathy and retinopathy. Fish & Shellfish Immunology, 53: 35–49. PMID: 26997200 DOI: 10.1016/j.fsi.2016.03.033

Duesund H, Nylund S, Watanabe K, Ottem KF and Nylund A. 2010. Characterization of a VHS virus genotype III isolated from rainbow trout (*Oncorhychus mykiss*) at a marine site on the west coast of Norway. Virology Journal, 7(1): 1–15.

Elston RA, Harrell L, and Wilkinson MT. 1986. Isolation and in vitro characteristics of chinook salmon (Oncorhynchus tshawytscha) rosette agent. Aquaculture, 56(1): 1–21. DOI: 10.1016/0044-8486(86)90286-3

Fringuelli E, Gordon AW, Rodger H, Welsh MD and Graham DA. 2012. Detection of Neoparamoeba perurans by duplex quantitative Taqman real-time PCR in formalin-fixed, paraffin-embedded Atlantic salmonid gill tissues. Journal of Fish Diseases, 35(10): 711–724.

Fukuwaka M, Sato S, and Takahashi S. 2007. Winter distribution of chum salmon related to environmental variables in the North Pacific. North Pacific. [online]: Available from researchgate.net/profile/Jamal_Moss/publication/266171339_Winter_Distribution_of_Chum_Salmon_Related_to_Environmental_Variables_in_the_North_Pacific/links/556f151d08aec226830a4f75/Winter-Distribution-of-Chum-Salmon-Related-to-Environmental-Variables-in-the-North-Pacific.pdf.

Garseth ÅH, Fritsvold C, Opheim M, Skjerve E, and Biering E. 2013. Piscine reovirus (PRV) in wild Atlantic salmon, Salmo salar L., and sea-trout, Salmo trutta L., in Norway. Journal of Fish Diseases, 36(5): 483–493.

Gozlan RE, Whipps CM, Andreou D, and Arkush KD. 2009. Identification of a rosette-like agent as Sphaerothecum destruens, a multi-host fish pathogen. International Journal for Parasitology, 39(10): 1055–1058. PMID: 19477179 DOI: 10.1016/j.ijpara.2009.04.012

Gu Z, Eils R, and Schlesner M. 2016. Complex heatmaps reveal patterns and correlations in multidimensional genomic data. Bioinformatics, 32(18): 2847–2849. PMID: 27207943 DOI: 10.1093/bioinformatics/btw313

Hallett SL and Bartholomew JL. 2006. Application of a real-time PCR assay to detect and quantify the myxozoan parasite Ceratomyxa shasta in river water samples. Diseases of Aquatic Organisms, 71(2): 109–118.

Hallett SL and Bartholomew JL. 2009. Development and application of a duplex QPCR for river water samples to monitor the myxozoan parasite Parvicapsula minibicornis. Diseases of Aquatic Organisms, 86(1): 39–50.

Hershberger PK, Stick K, Bui B, Carroll C, Fall B, Mork C, et al. 2002. Incidence of Ichthyophonus hoferi in Puget Sound fishes and its increase with age of Pacific herring. Journal of Aquatic Animal Health, 14(1): 50–56. DOI: 10.1577/1548-8667(2002)014<0050:IOIHIP>2.0.CO;2

Hinch SG, Healey MC, Diewert RE, Henderson MA, Thomson KA, Hourston R, and Juanes F. 1995. Potential effects of climate change on marine growth and survival of Fraser River sockeye salmon. Canadian Journal of Fisheries and Aquatic Sciences. Journal canadien des sciences halieutiques et aquatiques, 52(12): 2651–2659. DOI: 10.1139/f95-854

Holtby LB, Andersen BC, and Kadowaki RK. 1990. Importance of Smolt size and early ocean growth to interannual variability in Marine survival of Coho Salmon (Oncorhynchus kisutch). Canadian Journal of Fisheries and Aquatic Sciences. Journal canadien des sciences halieutiques et aquatiques, 47(11): 2181–2194. DOI: 10.1139/f90-243

Houde ALS, Akbarzadeh A, Günther OP, Li S, Patterson DA, Farrell AP, Hinch SG, and Miller KM. 2019. Salmonid gene expression biomarkers indicative of physiological responses to changes in salinity and temperature, but not dissolved oxygen. The Journal of Experimental Biology, 222(Pt 13). DOI: 10.1242/jeb.198036

Houde ALS, Günther OP, Strohm J, Ming TJ, Li S, Kaukinen KH, et al. 2019. Discovery and validation of candidate smoltification gene expression biomarkers across multiple species and ecotypes of Pacific salmonids. Conservation Physiology, 7(1): coz051. DOI: 10.1093/conphys/coz051

Irvine JR, and Akenhead SA. 2013. Understanding Smolt survival trends in Sockeye Salmon. Marine and Coastal Fisheries: Dynamics, Management, and Ecosystem Science, 5(1): 303–328. DOI: 10.1080/19425120.2013.831002

Ishida Y, Ueno Y, Nagasawa K, and Shiomoto A. 2000. 'Review of ocean salmon research by Japan from 1991 to 1998', Bulletin. North Pacific Anadromous Fish Commission, 2, pp. 191–201.

Jeffries KM, Hinch SG, and Sierocinski T. 2014. Transcriptomic responses to high water temperature in two species of Pacific salmon. Evolutionary. [online]: Available from onlinelibrary.wiley.com/doi/abs/10.1111/eva.12119.

Jensen J, and Ørntoft T. 2004. Normalization of real-time quantitative RT-PCR data: A model based variance estimation approach to identify genes suited for normalization-applied to bladder-and colon-cancer data-sets. Cancer Research, 64(5245): 50.

Jonstrup SP, Kahns S, Skall HF, Boutrup TS, and Olesen NJ. 2013. Development and validation of a novel T aqman-based real-time RT-PCR assay suitable for demonstrating freedom from viral haemorrhagic septicaemia virus. Journal of Fish Diseases, 36(1): 9–23.

Jørgensen A, Nylund A, Nikolaisen V, Alexandersen S, and Karlsbakk E. 2011. Real-time PCR detection of Parvicapsula pseudobranchicola (Myxozoa: Myxosporea) in wild salmonids in Norway. Journal of Fish Diseases, 34(5): 365–371.

Kendall NW, Marston GW, and Klungle MM. 2017. Declining patterns of Pacific Northwest steelhead trout (Oncorhynchus mykiss) adult abundance and smolt survival in the ocean. Canadian Journal of Fisheries and Aquatic Sciences. Journal canadien des sciences halieutiques et aquatiques, 74(8): 1275–1290. DOI: 10.1139/cjfas-2016-0486

Korsnes K, Devold M, Nerland AH, and Nylund A. 2005. Viral encephalopathy and retinopathy (VER) in Atlantic salmon Salmo salar after intraperitoneal challenge with a nodavirus from Atlantic halibut Hippoglossus hippoglossus. Diseases of Aquatic Organisms, 68(1): 7–16.

Krasnov A, Afanasyev S, Nylund S, and Rebl A. 2020. Multigene expression assay for assessment of the immune status of Atlantic Salmon. Genes, 11(11). DOI: 10.3390/genes11111236

Larionov A, Krause A, and Miller W. 2005. A standard curve based method for relative real time PCR data processing. BMC Bioinformatics, 6: 62. PMID: 15780134 DOI: 10.1186/1471-2105-6-62

Latshaw JD. 1991. Nutrition—mechanisms of immunosuppression. Veterinary Immunology and Immunopathology, 30(1): 111–120. PMID: 1781151 DOI: 10.1016/0165-2427(91)90012-2

Laurin E, Jaramillo D, Vanderstichel R, Ferguson H, Kaukinen K, Schulze AD, et al. 2019. Histopathological and novel high-throughput molecular monitoring data from farmed salmon (Salmo salar and Oncorhynchus spp.) in British Columbia, Canada, from 2011–2013. Aquaculture, 499: 220–234. DOI: 10.1016/j.aquaculture.2018.08.072

Lichatowich J, and Lichatowich JA. 2001. Salmon without rivers: A history of the Pacific Salmon crisis. Island Press.

Litzow MA, Ciannelli L, Puerta P, Wettstein JJ, Rykaczewski RR, and Opiekun M. 2018. Non-stationary climate–salmon relationships in the Gulf of Alaska. Proceedings of the Royal Society B: Biological Sciences, 285(1890): 20181855.

Livak KJ, and Schmittgen TD. 2001. Analysis of relative gene expression data using real-time quantitative PCR and the 2-$\Delta\Delta$CT method. Methods, 25(4): 402–408. PMID: 11846609 DOI: 10.1006/meth.2001.1262

Lloyd SJ, LaPatra SE, Snekvik KR, Cain KD, and Call DR. 2011. Quantitative PCR demonstrates a positive correlation between a Rickettsia-like organism and severity of strawberry disease lesions in rainbow trout, Oncorhynchus mykiss (Walbaum). Journal of Fish Diseases, 34(9): 701–709.

Lord GM, Matarese G, Howard JK, Baker RJ, Bloom SR, and Lechler RI. 1998. Leptin modulates the T-cell immune response and reverses starvation-induced immunosuppression. Nature, 394(6696): 897–901. PMID: 9732873 DOI: 10.1038/29795

Losee, JP, Fisher J, Teel DJ, Baldwin RE, Marcogliese DJ, and Jacobson KC. 2014. Growth and condition of juvenile coho salmon Oncorhynchus kisutch relate positively to species richness of trophically transmitted parasites. Journal of Fish Biology, 85(5): 1665–1681. PMID: 25271907 DOI: 10.1111/jfb.12525

Martin SA, Douglas A, Houlihan DF, and Secombes CJ. 2010. Starvation alters the liver transcriptome of the innate immune response in Atlantic salmon (Salmo salar). BMC Genomics, 11(1): 1–20.

Miller KM, Gardner IA, Vanderstichel R, Burnley T, Schulze AD, Li S, et al. 2016. Report on the performance evaluation of the Fluidigm BioMark platform for high-throughput microbe monitoring in salmon. researchgate.net. [online]: Available from researchgate.net/profile/Kristi_Miller3/publication/306281417_Report_on_the_Performance_Evaluation_of_the_Fluidigm_BioMark_Platform_for_High-Throughput_Microbe_Monitoring_in_Salmon/links/57b6565e08aede8a665bc0e5.pdf.

Miller KM, Günther OP, Li S, Kaukinen KH, and Ming TJ. 2017. Molecular indices of viral disease development in wild migrating salmon. Conservation Physiology, 5(1). [online] Available from: academic.oup.com/conphys/article-abstract/5/1/cox036/3896048. DOI: 10.1093/conphys/cox036

Miller KM, Li S, Kaukinen KH, Ginther N, Hammill E, Curtis JMR, et al. 2011. Genomic signatures predict migration and spawning failure in wild Canadian salmon. Science, 331(6014): 214–217. PMID: 21233388 DOI: 10.1126/science.1196901

Miller KM, Teffer A, Tucker S, Li S, Schulze AD, Trudel M, et al. 2014. Infectious disease, shifting climates, and opportunistic predators: Cumulative factors potentially impacting wild salmon declines. Evolutionary Applications, 7(7): 812–855. PMID: 25469162 DOI: 10.1111/eva.12164

Mitchell SO, Steinum TM, Toenshoff ER, and Kvellestad A. 2013. "Candidatus Branchiomonas cysticola" is a common agent of epitheliocysts in seawater-farmed Atlantic salmon Salmo salar in Norway and Ireland. Diseases of Aquatic Organisms, 103(1): 35–43. PMID: 23482383 DOI: 10.3354/dao02563

Mizuno S, Urawa S, Miyamoto M, Saneyoshi H, Hatakeyama M, Koide N, and Ueda H. 2017. Epizootiology of the ectoparasitic protozoans Ichthyobodo salmonis and Trichodina truttae on wild chum salmon Oncorhynchus keta. Diseases of Aquatic Organisms, 126(2): 99–109. PMID: 29044040 DOI: 10.3354/dao03162

Mordecai GJ, Di Cicco E, Gunther OP and Schulze AD. 2020. Emerging viruses in British Columbia salmon discovered via a viral immune response biomarker panel and metatranscriptomic sequencing. bioRxiv. DOI: 10.1101/2020.02.13.948026

Mordecai GJ, Miller KM, Di Cicco E, Schulze AD, Kaukinen KH, Ming TJ, et al. 2019. Endangered wild salmon infected by newly discovered viruses. eLife, 8. DOI: 10.7554/eLife.47615

NAGASAWA and K. 2000. Winter zooplankton biomass in the subarctic North Pacific, with discussion on the overwintering survival strategy of Pacific salmon (Oncorhynchus spp.). Bulletin. North Pacific Anadromous Fish Commission, 2: 21–32.

Naydenko SV, Temnykh OS, and Figurkin AL. 2016. Is winter the critical period in the marine life history of Pacific salmon? N. Bulletin. North Pacific Anadromous Fish Commission, 6: 139–152. DOI: 10.23849/npafcb6/139.152

Nekouei O, Vanderstichel R, Ming T, Kaukinen KH, Thakur K, Tabata A, et al. 2018. Detection and assessment of the distribution of infectious agents in Juvenile Fraser River Sockeye Salmon, Canada, in 2012 and 2013. Frontiers in Microbiology, 9: 3221. PMID: 30627126 DOI: 10.3389/fmicb.2018.03221

NOAA. 2021. Cold & warm episodes by season. [online]: Available from origin.cpc.ncep.noaa.gov/products/analysis_monitoring/ensostuff/ONI_v5.php.

Nylund A, Hansen H, Brevik ØJ, Hustoft H, Markussen T, Plarre H, and Karlsbakk E. 2018. Infection dynamics and tissue tropism of Parvicapsula pseudobranchicola (Myxozoa: Myxosporea) in farmed Atlantic salmon (Salmo salar). Parasites & Vectors, 11(1): 17. PMID: 29306320 DOI: 10.1186/s13071-017-2583-9

Nylund S, Nylund A, Watanabe K, Arnesen CE, and Karlsbakk E. 2010. Paranucleospora theridion n. gen., n. sp.(Microsporidia, Enterocytozoonidae) with a life cycle in the salmon louse (Lepeophtheirus salmonis, Copepoda) and Atlantic salmon (Salmo salar). The Journal of Eukaryotic Microbiology, 57(2): 95–114. PMID: 20070452 DOI: 10.1111/j.1550-7408.2009.00451.x

Nylund S, Steigen A, Karlsbakk E, Plarre H, Andersen L, Karlsen M, Watanabe K, and Nylund A. 2015. Characterization of "Candidatus Syngnamydia salmonis"(Chlamydiales, Simkaniaceae), a bacterium associated with epitheliocystis in Atlantic salmon (Salmo salar L.). Archives of Microbiology, 197(1): 17–25. PMID: 25294188 DOI: 10.1007/s00203-014-1038-3

Nylund A, Watanabe K, Nylund S, Karlsen M, Saether PA, Arnesen CE, and Karlsbakk E. 2008. Morphogenesis of salmonid gill poxvirus associated with proliferative gill disease in farmed Atlantic salmon (Salmo salar) in Norway. Archives of Virology, 153(7): 1299–1309.

Ogura M, and Ishida Y. 1992. Swimming behavior of coho salmon, Oncorhynchus kisutch, in the open sea as determined by ultrasonic telemetry. Canadian Journal of Fisheries and Aquatic Sciences. Journal canadien des sciences halieutiques et aquatiques, 49(3): 453–457. DOI: 10.1139/f92-053

Ogura M, and Ishida Y. 1995. Homing behavior and vertical movements of four species of Pacific salmon (Oncorhynchus spp.) in the central Bering Sea'. Canadian Journal of Fisheries and Aquatic Sciences. Journal canadien des sciences halieutiques et aquatiques, 52(3): 532–540. DOI: 10.1139/f95-054

Pagowski VA, Mordecai GJ, Miller KM, Schulze AD, Kaukinen KH, Ming TJ, et al. 2019. Distribution and phylogeny of Erythrocytic necrosis virus (ENV) in Salmon suggests marine origin. Viruses, 11(4). DOI: 10.3390/v11040358

Pakhomov EA, Deeg C, Esenkulova S, Foley G, Hunt BPV, Ivanov A, et al. 2019. Summary of preliminary findings of the International Gulf of Alaska expedition onboard the R/V Professor Kaganovskiy during February 16–March 18, 2019. NPAFC Doc., 1858: 25 pp.

Powell M, Overturf K, Hogge C, and Johnson K. 2005. Detection of Renibacterium salmoninarum in Chinook salmon, Oncorhynchus tshawytscha (Walbaum), using quantitative PCR. Journal of Fish Diseases, 28(10): 615–622.

Radchenko VI. 2006. The role of Pacific Salmon in the freshwater ecosystem. Bulletin 1 of Implementation of the 'Concept of the Far Eastern Basin Program for the Study of Pacific Salmon': 183–192. (In Russian).

Radchenko VI. 2012. Abundance dynamics of pink salmon (Oncorhynchus gorbuscha) as a structured process determined by many factors. North Pacific Anadromous Fish Commission Technical Report, 8: 14–18.

Radchenko VI, Somov AA, and Kanzeparova AN. 2019. Pacific salmon abundance and biomass in the Gulf of Alaska from NPAFC expedition data in winter 2019. Bulletin of Pacific Salmon Studies in the Far East, 14: 116–132.

Rand PS. 2002. Modeling feeding and growth in Gulf of Alaska sockeye salmon: Implications for high-seas distribution and migration. Marine Ecology Progress Series, 234: 265–280. DOI: 10.3354/meps234265

Ruckelshaus MH, Levin P, Johnson JB, and Kareiva P. 2003. The Pacific Salmon Wars: What science brings to the challenge of recovering species. Annual Review of. Ecology and Systematics, 33: 665–706. DOI: 10.1146/annurev.ecolsys.33.010802.150504

Shaw RW, Kent ML, and Adamson ML. 1998. Modes of transmission of Loma salmonae (Microsporidia). Diseases of Aquatic Organisms, 33(2): 151–156. PMID: 9722404 DOI: 10.3354/dao033151

Shaw RW, Kent ML, Brown AM, Whipps CM, Adamson ML. 2000. Experimental and natural host specificity of Loma salmonae (Microsporidia). Diseases of Aquatic Organisms, 40(2): 131–136. PMID: 10782347 DOI: 10.3354/dao040131

Shuntov VP, and Temnykh OS. 2011. Pacific salmon in marine and ocean ecosystems. TINRO Center, Vladivostok, Russia.

Shuntov VP, Temnykh OS, and Ivanov OA. 2017. On the persistence of stereotypes concerning the marine ecology of Pacific salmon (Oncorhynchus spp.). Russian Journal of Marine Biology, 43(7): 507–534. DOI: 10.1134/S1063074017070045

Shuntov VP, Temnykh OS, and Naydenko SV. 2019. More on the factors that limit the abundance of Pacific Salmon (Oncorhynchus spp., family Salmonidae) during the ocean phase of their life history. Russian Journal of Marine Biology, 45(7): 511–524. DOI: 10.1134/S106307401907006X

Siddon EC, Heintz RA, and Mueter FJ. 2013. Conceptual model of energy allocation in walleye pollock (Theragra chalcogramma) from age-0 to age-1 in the southeastern Bering Sea. Deep-Sea Research. Part II, Topical Studies in Oceanography, 94: 140–149. DOI: 10.1016/j.dsr2.2012.12.007

Somov AA, Khleborodov AS, Slabinsky AM, Hunt B, and Pakhomov EA. 2019. Feeding habits of Pacific salmon in the Gulf of Alaska in February–March 2019. Bulletin of Pacific Salmon Studies in the Far East, 14: 185–199.

Startsev AV, and Rassadnikov OA. 1997. Winter distribution of humpback salmon Oncorhynchus gorbuscha from the Sea of Okhotsk in the waters of the northern Pacific. Journal of Ichthyology, 37(4): 282–287.

Sterud E, Forseth T, Ugedal O, Poppe TT, Jørgensen A, Bruheim T, Fjeldstad H-P, and Mo TA. 2007. Severe mortality in wild Atlantic salmon Salmo salar due to proliferative kidney disease (PKD) caused

by Tetracapsuloides bryosalmonae (myxozoa). Diseases of Aquatic Organisms, 77(3): 191–198. PMID: 18062470 DOI: 10.3354/dao01846

Sutherland BJG, Hanson KC, Jantzen JR, Koop BF, and Smith CT. 2014. Divergent immunity and energetic programs in the gills of migratory and resident Oncorhynchus mykiss. Molecular Ecology, 23(8): 1952–1964. PMID: 24612010 DOI: 10.1111/mec.12713

Sveen S, Øverland H, Karlsbakk E, and Nylund A. 2012. Paranucleospora theridion (Microsporidia) infection dynamics in farmed Atlantic salmon Salmo salar put to sea in spring and autumn. Diseases of Aquatic Organisms, 101(1): 43–49. PMID: 23047190 DOI: 10.3354/dao02464

Teffer AK, Hinch SG, Miller KM, Patterson DA, Farrell AP, Cooke SJ, et al. 2017. Capture severity, infectious disease processes and sex influence post-release mortality of sockeye salmon bycatch,. Conservation Physiology, 5(1): cox017. DOI: 10.1093/conphys/cox017

Toenshoff ER, Kvellestad A, Mitchell SO, Steinum T, Falk K, Colquhoun DJ, and Horn M. 2012. A novel betaproteobacterial agent of gill epitheliocystis in seawater farmed Atlantic salmon (Salmo salar). PLoS ONE, 7(3): e32696. PMID: 22427865 DOI: 10.1371/journal.pone.0032696

Tucker S, Li S, Kaukinen KH, Patterson DA, and Miller KM. 2018. Distinct seasonal infectious agent profiles in life-history variants of juvenile Fraser River Chinook salmon: An application of high-throughput genomic screening. PLoS ONE, 13(4): e0195472. PMID: 29672620 DOI: 10.1371/journal.pone.0195472

Twardek WM, Chapman JM, Miller KM, Beere MC, Li S, Kaukinen KH, Danylchuk AJ, and Cooke SJ. 2019. Evidence of a hydraulically challenging reach serving as a barrier for the upstream migration of infection-burdened adult steelhead. Conservation Physiology, 7(1): coz023.

UENO and Y. 1999. Winter distribution and migration of Pacific salmon. Salmon Report Series, 48: 59–82.

Urawa, S. 1993. Effects of Ichthyobodo necator infections on seawater survival of juvenile chum salmon (Oncorhynchus keta). Aquaculture, 110(2): 101–110. DOI: 10.1016/0044-8486(93)90264-Y

Urawa S, Irvine JR, Kim JK, and Volk E. 2016. Forecasting Pacific salmon production in a changing climate: A review of the 2011–2015 NPAFC science plan. Bulletin. North Pacific Anadromous Fish Commission, 6: 501–534. DOI: 10.23849/npafcb6/501.534

Urawa S, Sato S, Crane PA, Agler B, Josephson R, and Azumaya T. 2009. Stock-specific ocean distribution and migration of chum salmon in the Bering Sea and North Pacific Ocean. Bulletin. North Pacific Anadromous Fish Commission, 5: 131–146.

Wang Y. 2018. The physiological associations between infectious agents and migrating juvenile Chinook salmon (Oncorhynchus Tshawytscha) (Doctoral dissertation, University of British Columbia).

Welch DW, Chigirinsky AI, and Ishida Y. 1995. Upper thermal limits on the oceanic distribution of Pacific salmon (Oncorhynchus spp.) in the spring. Canadian Journal of Fisheries and Aquatic Sciences. Journal canadien des sciences halieutiques et aquatiques, 52(3): 489–503. DOI: 10.1139/f95-050

White VC, Morado JF, Crosson LM, Vadopalas B, and Friedman CS. 2013. Development and validation of a quantitative PCR assay for Ichthyophonus spp. Diseases of Aquatic Organisms, 104(1): 69–81.

Wood CC, Rutherford DT, and McKinnell S. 1989. Identification of Sockeye Salmon (Oncorhynehus nerka) Stocks in Mixed-stock Fisheries in British Columbia and Southeast Alaska using Biological Markers. Canadian Journal of Fisheries and Aquatic Sciences. Journal canadien des sciences halieutiques et aquatiques, 46(12): 2108–2120. DOI: 10.1139/f89-261

Woodey JC. 1987. In-season management of Fraser River sockeye salmon (Oncorhynchus nerka): Meeting multiple objectives. Sockeye Salmon: 367–374.

Yokoyama H, Grabner D, and Shirakashi S. 2012. Transmission biology of the Myxozoa. *In* Health and environment in aquaculture. *Edited by* ED Carvalho, GS David, RJ Silva. InTech, Croatia. pp. 1–42.

Zimmerman MS, Irvine JR, O'Neill M, Anderson JH, Greene CM, Weinheimer J, Trudel M, and Rawson K. 2015. Spatial and temporal patterns in Smolt survival of wild and Hatchery Coho Salmon in the Salish Sea. Marine and Coastal Fisheries: Dynamics, Management, and Ecosystem Science, 7(1): 116–134. DOI: 10.1080/19425120.2015.1012246